
PROJECTION-FREE COMPUTATION OF ROBUST CONTROLLABLE SETS WITH CONSTRAINED ZONOTOPES

A PREPRINT

Abraham P. Vinod*, Avishai Weiss, and Stefano Di Cairano
 Mitsubishi Electric Research Laboratories, Cambridge, MA 02139
 abraham.p.vinod@ieee.org, weiss@merl.com, dicairano@ieee.org

ABSTRACT

We study the problem of computing robust controllable sets for discrete-time linear systems with additive uncertainty. We propose a tractable and scalable approach to inner- and outer-approximate robust controllable sets using constrained zonotopes, when the additive uncertainty set is a symmetric, convex, and compact set. Our least-squares-based approach uses novel closed-form approximations of the Pontryagin difference between a constrained zonotopic minuend and a symmetric, convex, and compact subtrahend. Unlike existing approaches, our approach does not rely on convex optimization solvers, and is projection-free for ellipsoidal and zonotopic uncertainty sets. We also propose a least-squares-based approach to compute a convex, polyhedral outer-approximation to constrained zonotopes, and characterize sufficient conditions under which all these approximations are exact. We demonstrate the computational efficiency and scalability of our approach in several case studies, including the design of abort-safe rendezvous trajectories for a spacecraft in near-rectilinear halo orbit under uncertainty. Our approach can inner-approximate a 20-step robust controllable set for a 100-dimensional linear system in under 15 seconds on a standard computer.

1 Introduction

Robust controllable (RC) sets characterize a set of states from which a collection of possibly time-varying state constraints can be satisfied by a controlled state trajectory, under bounded control authority and uncertainty. RC sets are essential for robust model predictive control [1–5], fault-tolerant control [6–8], and verification of dynamical systems [9–12], and have been used in a broad range of applications in space [10–13], transportation [14], and robotics [15, 16]. For discrete-time linear systems with additive uncertainty and bounded, polytopic state and input constraints, exact RC sets are known to be polytopes, and the RC sets may be computed using set computations on polytopes. However, polytope-based RC set computation involves projection that has a combinatorial computational complexity and causes numerical issues for high-dimensional systems and/or over long horizons [3, 15, 17]. In this paper, we focus in addressing these shortcomings, and propose *novel theory and algorithms for efficient and scalable computation of inner- and outer-approximations of RC sets, that admit closed-form description of the sets involved and can be computed without relying on convex optimization solvers in several cases.*

We are motivated by the problem of designing *active, abort-safe, spacecraft rendezvous* trajectories with the Lunar gateway [18]. In abort-safe rendezvous, we seek rendezvous trajectories that nominally steer the control-constrained spacecraft towards the rendezvous target, while allowing for the possibility of diverting away from the rendezvous target in the event of failure. Often, failures in space applications are characterized by partial or complete loss of actuation, and increased actuation and navigational uncertainties that may appear as additive uncertainties in the dynamics. For designing such rendezvous trajectories, we use RC sets to characterize a set of state constraints that a nominal trajectory should satisfy, where the RC sets encode the desirable property of safe abort under limited available actuation and uncertainty, similarly to [11, 13]. However, polytope-based computation of RC sets for high-dimensional systems suffers from numerical issues, primarily due to projection [3, 15, 17]. On the other hand, our approach can efficiently compute the required high-dimensional RC sets.

*Corresponding author

We will use constrained zonotopes, a recently proposed alternative description to polytopes [6, 7, 9, 19], to achieve tractable approximation of RC sets. In the disturbance-free setting, constrained zonotopes provide closed-form expressions for all set operations used in the exact computation of the *controllable set* [6]. However, an exact computation of RC sets using constrained zonotopes is hindered by the fact that there are no tractable approaches to compute the exact Pontryagin difference with a constrained zonotopic minuend [7, 9].

Recently, [9] described an optimization-based two-stage approach to inner-approximate the Pontryagin difference between a constrained zonotope and a zonotope, which allows for computing inner-approximations of RC sets when the additive disturbance set is a zonotope. However, it is unclear how such an approach extends to ellipsoidal uncertainty (a more common setting in control), and the reliance of optimization hinders fast computation of RC sets for high-dimensional systems. In this paper, we propose *least-squares-based algorithms to generate constrained zonotopes that inner- and outer-approximate the Pontryagin difference between a constrained zonotopic minuend and a symmetric, convex, and compact subtrahend*. Our approaches also admit closed-form expressions for the approximations when using a full-dimensional minuend, and an ellipsoidal or zonotopic subtrahend. Then, we use these algorithms for fast and scalable computation of RC sets for an additive uncertainty set that is symmetric, convex, and compact.

The main contributions of this paper are as follows: 1) a tractable inner- and outer-approximation of the Pontryagin difference between a constrained zonotopic minuend and a symmetric, convex, and compact subtrahend, 2) an inner- and outer-approximation of the RC sets using the proposed approximations to the Pontryagin difference, 3) a closed-form description of a polyhedral outer-approximation of a constrained zonotope, and 4) sufficient conditions under which the approximations proposed above are exact. All of our approaches utilize least-squares method as the primary tool for which efficient implementations are widely available [20], and does not typically rely on convex optimization solvers as required in [9]. Additionally, the proposed approximations to the Pontryagin difference admit closed-form expressions when the subtrahend is an ellipsoid, a zonotope, or a convex hull of a collection of symmetric intervals. These features together enable an inner-approximation of a 20-step RC set for a 100-dimensional linear system in less than 15 seconds on a standard computer.

The rest of this paper is organized as follows: Section 2 provides the necessary mathematical background and states the problem statements of interest. Sections 3 and 4 describe the proposed approaches to approximate the Pontryagin difference between a constrained zonotopic minuend and a symmetric, convex, and compact subtrahend respectively. Section 5 applies these approaches to the computation of RC sets, and Section 6 presents several case studies that demonstrate the utility and scalability of the proposed approach. Section 7 applies the method to the (simplified) motivating problem of active abort-safe rendezvous with the Lunar gateway. Section 8 summarizes the paper.

2 Preliminaries

$0_{n \times m}$ and $1_{n \times m}$ are matrices of zeros and ones in $\mathbb{R}^{n \times m}$ respectively, I_n is the n -dimensional identity matrix, $\mathbb{N}_{[a:b]}$ is the subset of natural numbers between (and including) $a, b \in \mathbb{N}$, $a \leq b$, e_i is the standard axis vectors of \mathbb{R}^n , and $\|\cdot\|_p$ is the ℓ_p -norm of a vector. Let M be a matrix and M_1 (M_2 , resp.) be another matrix of the same height (width, resp.) as M . Then, $[M, M_1]$ ($[M; M_2]$, resp.) denotes the matrix obtained by concatenating M and M_1 horizontally (concatenating M and M_2 vertically, resp.). For a matrix $M \in \mathbb{R}^{m \times n}$ with full row rank, $M^\dagger = M^\top (MM^\top)^{-1}$ denotes its (right) pseudoinverse, and $x = M^\dagger v$ solves the system of linear equation $Mx = v$ for any vector $v \in \mathbb{R}^m$ [20, Sec. 11.5]. Given a vector $d \in \mathbb{R}^n$, $\text{diag}(d)$ is a n -dimensional diagonal matrix with d_i as its diagonal entries.

A set $\mathcal{S} \subset \mathbb{R}^n$ is said to be *symmetric* about any $c \in \mathbb{R}^n$, if $c + x \in \mathcal{S}$ implies $c - x \in \mathcal{S}$ for any $x \in \mathbb{R}^n$. For any set $\mathcal{S} \subseteq \mathbb{R}^n$, we denote its *convex hull* and *affine hull* by $\text{CH}(\mathcal{S})$ and $\text{AH}(\mathcal{S})$ respectively. Recall that $\text{AH}(\mathcal{S})$ is an affine set such that $\mathcal{S} \subseteq \mathcal{A} \Rightarrow \text{AH}(\mathcal{S}) \subseteq \mathcal{A}$ for any affine set \mathcal{A} . The *affine dimension* of a set \mathcal{S} is the dimension of the subspace associated with $\text{AH}(\mathcal{S})$. A *full-dimensional* set in \mathbb{R}^n is a non-empty set with an affine dimension of n . See [21, Sec. 2.1] for more details.

2.1 Set representations

Let $\mathcal{P}, \mathcal{C}, \mathcal{I}, \mathcal{Z}$, and \mathcal{E} be convex and compact sets in \mathbb{R}^n . Then, \mathcal{P} is a *convex polytope* if (1a) holds; \mathcal{C} is a *constrained zonotope* if (1b) holds; \mathcal{I} is a *convex union of symmetric intervals* if (1c) holds; \mathcal{Z} is a *zonotope* if (1d) holds; and \mathcal{E} is an *ellipsoid* if (1e) holds:

$$\exists(H_P, k_P) \in \mathbb{R}^{N_P \times n} \times \mathbb{R}^{N_P} : \mathcal{P} = \{x : H_P x \leq k_P\}, \quad (1a)$$

$$\exists(G_C, c_C, A_C, b_C) \in \mathbb{R}_C : \mathcal{C} = \{G_C \xi + c_C : \|\xi\|_\infty \leq 1, A_C \xi = b_C\}, \quad (1b)$$

$$\exists(G_I, c_I) \in \mathbb{R}^{n \times N_I} \times \mathbb{R}^n : \mathcal{I} = \{G_I \xi + c_I : \|\xi\|_1 \leq 1\}, \quad (1c)$$

$$\exists(G_Z, c_Z) \in \mathbb{R}^{n \times N_Z} \times \mathbb{R}^n : \mathcal{Z} = \{G_Z \xi + c_Z : \|\xi\|_\infty \leq 1\}, \quad (1d)$$

$$\exists(G_E, c_E) \in \mathbb{R}^{n \times n} \times \mathbb{R}^n : \mathcal{E} = \{G_E \xi + c_E : \|\xi\|_2 \leq 1\}, \quad (1e)$$

where $\mathbb{R}_C \triangleq \mathbb{R}^{n \times N_C} \times \mathbb{R}^n \times \mathbb{R}^{M_C \times N_C} \times \mathbb{R}^{M_C}$. We refer to *unbounded* convex sets in (1a) as *convex polyhedra*.

Zonotopes \mathcal{Z} , ellipsoids \mathcal{E} , and convex unions of symmetric intervals \mathcal{I} are affine transformations of unit balls defined using ℓ_∞ -norms, ℓ_2 -norms, and ℓ_1 -norms respectively, and are symmetric about c_Z , c_E , and c_I respectively in (1d), (1e), and (1c). Specifically, by the definition of ℓ_1 -norm, \mathcal{I} is the convex hull of the union of symmetric intervals defined by the columns of $G_I = [g_1, g_2, \dots, g_{N_I}]$,

$$\mathcal{I} = c_I + \text{CH} \left(\bigcup_{j \in \mathbb{N}_{[1:N_I]}} [-g_j, g_j] \right), \quad (2)$$

where $[-g, g] = \{g\theta : -1 \leq \theta \leq 1\}$ denotes an *interval*.

From [6, Thm. 1], every convex polytope \mathcal{P} can be represented as a constrained zonotope \mathcal{C} , and vice versa. Additionally, [6, Thm. 1] provides a systematic approach to convert \mathcal{P} in the form of (1a) to a constrained zonotope \mathcal{C} in the form of (1b). However, converting \mathcal{C} to \mathcal{P} exactly is known to be a computationally demanding process, with existing approaches applicable only for low-dimensional constrained zonotopes [6, Prop. 3].

From (1b), a constrained zonotope \mathcal{C} can also be interpreted as the image of a linearly-constrained unit-hypercube $\mathcal{B}_\infty(A_C, b_C)$ under an affine mapping defined by (G_C, c_C) , i.e., $\mathcal{C} = c_C + G_C \mathcal{B}_\infty(A_C, b_C)$ where

$$\mathcal{B}_\infty(A_C, b_C) \triangleq \{\xi : \|\xi\|_\infty \leq 1, A_C \xi = b_C\}. \quad (3)$$

In (3), $\mathcal{B}_\infty(A_C, b_C)$ is the intersection of a unit-hypercube in \mathbb{R}^{N_C} and M_C linear equalities. By definition, $\mathcal{C} \neq \emptyset$ if and only if $\mathcal{B}_\infty(A_C, b_C) \neq \emptyset$.

Definition 1. (REPRESENTATION COMPLEXITY) *The representation complexity of a constrained zonotope \mathcal{C} is $\mathcal{C}(\mathcal{C}) = (n, N_C, M_C)$.*

The complexity $\mathcal{C}(\mathcal{C})$ is not unique, since the representation (1b) is not unique, e.g., adding redundant equality constraints to (A_C, b_C) does not alter \mathcal{C} . We compare representation complexities for sets with identical dimensions n using componentwise inequalities. Specifically, for two constrained zonotopes $\mathcal{C}_1, \mathcal{C}_2$, we have $\mathcal{C}(\mathcal{C}_1) \preceq \mathcal{C}(\mathcal{C}_2)$ if and only if $N_{C_1} \leq N_{C_2}$ and $M_{C_1} \leq M_{C_2}$.

For a convex and compact set $\mathcal{S} \subset \mathbb{R}^n$, its support function $\rho : \mathbb{R}^n \rightarrow \mathbb{R}$ and support vector $\vartheta : \mathbb{R}^n \rightarrow \mathbb{R}^n$ are

$$\vartheta_{\mathcal{S}}(\nu) = \arg \sup_{s \in \mathcal{S}} \nu^\top s, \text{ and } \rho_{\mathcal{S}}(\nu) = \nu^\top \vartheta_{\mathcal{S}}(\nu). \quad (4)$$

Using *dual norms* [21, Sec. A.1.6] and properties of support function [22, Prop. 2], we have closed-form expressions for the support function of zonotopes \mathcal{Z} , ellipsoids \mathcal{E} , and convex unions of symmetric intervals \mathcal{I} ,

$$\rho_{\mathcal{I}}(\nu) = \nu^\top c_I + \|G_I^\top \nu\|_\infty, \quad (5a)$$

$$\rho_{\mathcal{E}}(\nu) = \nu^\top c_E + \|G_E^\top \nu\|_2, \quad (5b)$$

$$\rho_{\mathcal{Z}}(\nu) = \nu^\top c_Z + \|G_Z^\top \nu\|_1. \quad (5c)$$

2.2 Set operations

For any sets $\mathcal{C}, \mathcal{S} \subseteq \mathbb{R}^n$ and $\mathcal{W} \subseteq \mathbb{R}^m$, and a matrix $R \in \mathbb{R}^{m \times n}$, we define the set operations (affine map, Minkowski sum \oplus , intersection with inverse affine map \cap_R , and Pontryagin difference \ominus):

$$R\mathcal{C} \triangleq \{Ru : u \in \mathcal{C}\}, \quad (6a)$$

$$\mathcal{C} \oplus \mathcal{S} \triangleq \{u + v : u \in \mathcal{C}, v \in \mathcal{S}\}, \quad (6b)$$

$$\mathcal{C} \cap_R \mathcal{W} \triangleq \{u \in \mathcal{C} : Ru \in \mathcal{W}\}, \quad (6c)$$

$$\mathcal{C} \ominus \mathcal{S} \triangleq \{u : \forall v \in \mathcal{S}, u + v \in \mathcal{C}\}. \quad (6d)$$

Since $\mathcal{C} \cap \mathcal{S} = \mathcal{C} \cap_{I_n} \mathcal{S}$, (6c) also includes the standard intersection. For any $x \in \mathbb{R}^n$, we use $\mathcal{C} + x$ and $\mathcal{C} - x$ to denote $\mathcal{C} \oplus \{x\}$ and $\mathcal{C} \oplus \{-x\}$ respectively for brevity.

Constrained zonotopes admit closed-form expressions for various set operations described in (6). From [6, Prop. 1] and [7, Sec. 3.2],

$$RC = (RG_C, Rc_C, A_C, b_C), \quad (7a)$$

$$\mathcal{C} \oplus \mathcal{S} = ([G_C, G_S], c_C + c_S, [A_C, 0; 0, A_S], [b_C; b_S]), \quad (7b)$$

$$\mathcal{C} \cap_R \mathcal{W} = ([G_C, 0], c_C, [A_C, 0; 0, A_W; RG_C, -G_W], [b_C; b_W; c_W - Rc_C]), \quad (7c)$$

$$\mathcal{C} \cap \mathcal{H} = ([G_C, 0], c_C, [A_C, 0; p^\top G_C, d_m/2], [b_C; (q + p^\top c_C - \|p^\top G_C\|_1)/2]), \quad (7d)$$

where $\mathcal{H} = \{x : p^\top x \leq q\} \subset \mathbb{R}^n$ is an halfspace, and (7d) also enables an exact computation of the intersection of a constrained zonotope and a convex polyhedron.

To the best of our knowledge, no closed-form expression similar to (7) is available for the Pontryagin difference (6d). On the other hand, $\mathcal{P} \ominus \mathcal{S}$ for a convex polyhedral minuend \mathcal{P} (1a) defined by N_P linear constraints and a convex and compact subtrahend \mathcal{S} is given by

$$\mathcal{P} \ominus \mathcal{S} = \{x : H_P x \leq k_P - [\rho_S(h_1); \dots; \rho_S(h_{N_P})]\}, \quad (8)$$

with $H_P = [h_1^\top; h_2^\top; \dots; h_{N_P}^\top]$ [23, Thm. 2.3]. A direct use of (8) to implement $\mathcal{C} \ominus \mathcal{S}$ is prevented by the difficulty in converting \mathcal{C} in the form of (1b) to (1a).

Recently, [9] proposed a two-stage approach to inner-approximate $\mathcal{C} \ominus \mathcal{S}$ between a constrained zonotopic minuend \mathcal{C} and a zonotopic subtrahend \mathcal{S} with $G_S = [g_S^{(1)}, \dots, g_S^{(N_S)}]$. The two-stage approach first solves a linear program with $2N_C N_S$ variables,

$$\begin{aligned} & \text{minimize} && \text{SumAbs}(\Gamma) \\ & \text{s. t.} && [G_C; A_C]\Gamma = [G_S; 0_{M_C \times N_S}], \\ & && \forall i \in \mathbb{N}_{[1:N_C]}, \quad \sum_{j=1}^{N_S} |\Gamma_{ij}| \leq 1, \end{aligned} \quad (9)$$

where $\text{SumAbs}(\Gamma) \triangleq \sum_{i=1}^{N_C} \sum_{j=1}^{N_S} |\Gamma_{ij}|$. Let the optimal solution to (9) be Γ^* , if it exists, and the second stage defines a diagonal matrix $D \in \mathbb{R}^{N_C \times N_C}$ with

$$D_{ii} = 1 - \|e_i^\top \Gamma^*\|_1 = 1 - \sum_{j=1}^{N_S} |\Gamma_{ij}^*| \quad (10)$$

for each $i \in \mathbb{N}_{[1:N_C]}$. Then, a constrained zonotopic inner-approximation of $\mathcal{C} \ominus \mathcal{S}$ is

$$\mathcal{M}^- \triangleq (G_C D, c_C - c_S, A_C D, b_C) \subseteq \mathcal{C} \ominus \mathcal{S}. \quad (11)$$

The representation complexity of \mathcal{M}^- is identical to \mathcal{C} , which is a desirable feature when using (11) in set recursions involving the Pontryagin difference. However, solving (9) repeatedly can become computationally expensive for large N_C and/or N_S . Additionally, it is unclear if such an approach extends to subtrahends beyond zonotopes, since it uses polytopic containment results from [24]. We address these shortcomings in this paper.

Problem 1. Let \mathcal{C} be a constrained zonotope and \mathcal{S} be a convex and compact set that is symmetric about $c_S \in \mathbb{R}^n$. Characterize constrained zonotopes $\mathcal{M}^-, \mathcal{M}^+ \subset \mathbb{R}^n$ with

$$\mathcal{M}^- \subseteq \mathcal{M} \triangleq \mathcal{C} \ominus \mathcal{S} \subseteq \mathcal{M}^+, \quad (12)$$

where \mathcal{M}^- is available in closed-form, and the representation complexity of \mathcal{M}^- and \mathcal{C} are identical. Also, provide sufficient conditions for $\mathcal{M}^- = \mathcal{M} = \mathcal{M}^+$.

Our approach to address Problem 1 follows a similar two-stage approach to that in [9] to obtain (11). However, unlike [9], we provide closed-form expressions for Γ and D used in (10) and (11) for a broader class of subtrahends that includes ellipsoids and convex unions of symmetric intervals. We also propose a constrained zonotopic outer-approximation to \mathcal{M} , and provide sufficient conditions under which these approximations are exact. The proposed outer-approximation relies on solving the following problem.

Problem 2. Given a constrained zonotope \mathcal{C} , design an algorithm to compute an outer-approximating convex polyhedron \mathcal{P} (i.e., $\mathcal{P} \supseteq \mathcal{C}$) in the form of (1a) that has at most $2N_C$ linear constraints. Also, provide sufficient conditions under which $\mathcal{C} = \mathcal{P}$.

We will also briefly explore the connections between our proposed optimization-free two-stage approach and the optimization-based two-stage approach in [9].

2.3 Robust controllable set

Consider a linear time-varying system,

$$x_{t+1} = A_t x_t + B_t u_t + F_t w_t, \quad (13)$$

with state $x_t \in \mathbb{R}^n$, input $u_t \in \mathcal{U}_t \subset \mathbb{R}^m$, disturbance $w_t \in \mathcal{W}_t \subset \mathbb{R}^p$, and appropriately defined time-varying matrices A_t , B_t , and F_t .

Definition 2. (*T-STEP RC SET*) [3, DEFN. 10.18] *Given (13), a set of (possibly time-varying) state constraints $\{\mathcal{X}_t\}_{t=0}^{T-1}$ with $\mathcal{X}_t \subseteq \mathbb{R}^n$ for each t , and a goal set $\mathcal{G} \subset \mathbb{R}^n$, the T -step robust controllable (RC) set is*

$$\mathcal{K} = \{x_0 \in \mathcal{X}_0 \mid \forall t \in \mathbb{N}_{[0:T-1]}, \exists u_t \in \mathcal{U}_t, \forall w_t \in \mathcal{W}_t, x_{t+1} = A_t x_t + B_t u_t + F_t w_t, x_t \in \mathcal{X}_t, x_T \in \mathcal{G}\}.$$

Informally, the T -step RC set $\mathcal{K} \subset \mathbb{R}^n$ is the set of initial states that, despite the additive disturbance $w_t \in \mathcal{W}_t$, can be steered using $u_t \in \mathcal{U}_t$ to reach the goal set \mathcal{G} at time step T , while staying within the sequence of state constraints $\{\mathcal{X}_t\}_{t=0}^{T-1}$ at all intermediate time steps. The T -step RC set is also known in the literature as robust reachability of target tube [5], backward reachable set [9], or backward reach-avoid set [10]. We can compute \mathcal{K} via a set recursion,

$$\mathcal{K}_t = \text{Pre}(\mathcal{K}_{t+1}) \cap \mathcal{X}_t, \quad \forall t \in \mathbb{N}_{[0:T-1]}, \quad (14a)$$

$$\text{Pre}(\mathcal{K}_{t+1}) \triangleq \{x : A_t x \in (\mathcal{K}_{t+1} \ominus F_t \mathcal{W}) \oplus (-B_t \mathcal{U})\}, \quad (14b)$$

with $\mathcal{K}_T \triangleq \mathcal{G}$ and $\mathcal{K} = \mathcal{K}_0$. Observe that (14) uses all set operations in (6). For convex polyhedral/polytopic $\mathcal{X}, \mathcal{G}, \mathcal{S}, \mathcal{U}$, and \mathcal{W} , we can compute RC sets using polyhedral computational geometry [3, 4, 10]. However, we typically face numerical challenges when implementing (14) using polytopes for high-dimensional systems (13), or over long horizons T , primarily due to projection required by the combination of Minkowski sum and intersection operations [3, 15].

On the other hand, constrained zonotopes provide a tractable, exact solution when $\mathcal{W} = \emptyset$ using (7) [6, 7, 9]. Additionally, for a zonotopic \mathcal{W} , [9] uses the two-stage approach reviewed in Section 2.2 to propose an inner-approximation of \mathcal{K} . In this paper, we use our solution to Problem 1 to inner-approximate \mathcal{K} for a broader class of disturbance sets \mathcal{W} that are symmetric, convex, and compact.

Problem 3. *Compute a constrained zonotopic \mathcal{K}^- that inner-approximates \mathcal{K} defined in Definition 2, where for every $t \in \mathbb{N}_{[0:T-1]}$, \mathcal{U}_t and \mathcal{G} are convex polytopes, \mathcal{W}_t are symmetric, convex, and compact sets, and either 1) \mathcal{X}_t are convex polyhedra and A_t are invertible, or 2) \mathcal{X}_t are convex polytopes. Additionally, characterize the representation complexity of \mathcal{K}^- in both cases.*

In both settings considered, the exact RC sets are known to be polytopes [3], and hence are representable via constrained zonotopes. We also use the proposed outer-approximation to the Pontryagin difference to outer-approximate \mathcal{K}_t when using (14).

3 Inner-approximation of Pontryagin difference

Given a constrained zonotopic minuend $\mathcal{C} \subset \mathbb{R}^n$ and a symmetric, convex, and compact subtrahend $\mathcal{S} \subset \mathbb{R}^n$, we address the inner-approximation part of Problem 1 by characterizing a constrained zonotope,

$$\mathcal{M}^- \subseteq \mathcal{M} \triangleq \mathcal{C} \ominus \mathcal{S}. \quad (15)$$

Specifically, we provide closed-form expressions for a diagonal matrix $D \in \mathbb{R}^{N_C \times N_C}$ using the properties of \mathcal{C} and \mathcal{S} , and define $\mathcal{M}^- = (G_{M^-}, c_{M^-}, A_{M^-}, b_{M^-})$ with

$$G_{M^-} = G_C D, \quad c_{M^-} = c_C - c_S, \quad A_{M^-} = A_C D, \quad b_{M^-} = b_C, \quad (16a)$$

for a specific $c_S \in \mathcal{S}$, similarly to (11). By construction, the representation complexity of \mathcal{M}^- is $\mathcal{C}(\mathcal{M}^-) = (n, N_C, M_C) = \mathcal{C}(\mathcal{C})$.

We now state a mild assumption on the minuend \mathcal{C} that we will use to compute \mathcal{M}^- .

Assumption 1. *The minuend \mathcal{C} is full-dimensional.*

Observe that Assumption 1 on the minuend \mathcal{C} is not restrictive, as illustrated with the following two observations. First, $\mathcal{C} \ominus \mathcal{S} = \emptyset$, whenever the affine dimension of \mathcal{S} is strictly greater than the affine dimension of \mathcal{C} by (6d), since $x + \mathcal{S}$ can not be contained in \mathcal{C} for any $x \in \mathbb{R}^n$ in such a scenario. Second, consider the case where both minuend

| Subtrahend \mathcal{S} | Definition of the diagonal matrix $D = \text{diag}_{i \in \mathbb{N}_{[1:N_C]}}(D_{ii})$ | Result |
|--|--|---------|
| Convex and compact \mathcal{S} that is symmetric about $c_S \in \mathbb{R}^n$ | $D_{ii} = 1 - \rho_{\mathcal{S}_0}(e_i^\top [G_C; A_C]^\top [I_n; 0_{M_C \times n}])$ for $\mathcal{S}_0 \triangleq \mathcal{S} - c_S$ | Thm. 2 |
| Convex union of symmetric intervals (1c) $\mathcal{S} = \{G_S \xi + c_S : \ \xi\ _1 \leq 1\}$ | $D_{ii} = 1 - \ e_i^\top [G_C; A_C]^\top [G_S; 0_{M_C \times N_S}]\ _\infty$ | Corr. 1 |
| Zonotope (1d) $\mathcal{S} = \{G_S \xi + c_S : \ \xi\ _\infty \leq 1\}$ | $D_{ii} = 1 - \ e_i^\top [G_C; A_C]^\top [G_S; 0_{M_C \times N_S}]\ _1$ | |
| Ellipsoid (1e) $\mathcal{S} = \{G_S \xi + c_S : \ \xi\ _2 \leq 1\}$ | $D_{ii} = 1 - \ e_i^\top [G_C; A_C]^\top [G_S; 0_{M_C \times n}]\ _2$ | |

Table 1: Summary of the closed-form expressions for the diagonal matrix $D = \text{diag}_{i \in \mathbb{N}_{[1:N_C]}}(D_{ii})$ for various subtrahends \mathcal{S} that is symmetric about $c_S \in \mathbb{R}^n$, and the corresponding result in the paper. Given a full-dimensional constrained zonotopic minuend $\mathcal{C} = (G_C, c_C, A_C, b_C)$, we propose a constrained zonotope $\mathcal{M}^- = (G_C D, c_C - c_S, A_C D, b_C)$ that satisfies $\mathcal{M}^- \subseteq \mathcal{M} = \mathcal{C} \ominus \mathcal{S}$.

and subtrahend are not full-dimensional and there exists a matrix $T \in \mathbb{R}^{n \times n'}$ with $n > n'$ and $\text{rank}(T) = n'$ such that $\mathcal{C} = TC'$ and $\mathcal{S} = TS'$ for any $C', S' \subset \mathbb{R}^{n'}$. Then, by [23, Thm. 2.1.viii],

$$\mathcal{C} \ominus \mathcal{S} = (TC') \ominus (TS') = T(C' \ominus S'). \quad (17)$$

In such a case, it suffices to assume that C' is full-dimensional in order to inner-approximate $\mathcal{C} \ominus \mathcal{S}$.

We first show that Assumption 1 enables an equivalent representation of the minuend. We then address the inner-approximation part of Problem 1, and conclude the section by relating our approach with the two-stage approach in [9] for zonotopic subtrahends. Table 1 summarizes the computation of D for various types of sets considered in this paper.

3.1 MINROW representation for constrained zonotopes

We now show that Assumption 1 enables a useful, equivalent representation for a constrained zonotope (1b).

Definition 3. (MINROW REPRESENTATION) *A constrained zonotope $\mathcal{C} = (G_C, c_C, A_C, b_C)$ has a MINROW representation when $[G_C; A_C]$ has full row rank.*

A constrained zonotope (1b) in MINROW representation ensures that the matrix $[G_C; A_C]$ has a well-defined right pseudoinverse $[G_C; A_C]^\dagger$. However, the MINROW representation for a constrained zonotope is not unique, since one can preserve the rank of $[G_C; A_C]$ without altering \mathcal{C} by appropriately modifying G_C and A_C (e.g., increase N_C by adding columns of zeros to G_C and A_C).

Proposition 1. (RANK IMPLICATIONS) *Let Assumption 1 hold. Then, G_C has full row rank, and \mathcal{C} has a MINROW representation.*

See Appendix A.1 for the proof of Proposition 1.

Computing a MINROW representation of a full-dimensional constrained zonotope \mathcal{C} : By Proposition 1, a full-dimensional \mathcal{C} does not have a MINROW representation only if A_C has linearly dependent rows. For such a set \mathcal{C} , $[A_C, b_C]$ must also have linearly dependent rows since \mathcal{C} is non-empty (see Appendix A.1 for more details). We compute a MINROW representation of \mathcal{C} in the form of $\mathcal{C} = (G_C, c_C, A'_C, b'_C)$, where $[A'_C, b'_C]$ is a set of linearly independent rows of the matrix $[A_C, b_C]$ such that $\text{rank}([A'_C, b'_C]) = \text{rank}([A_C, b_C])$. The rest of the paper assumes that a MINROW representation is used whenever a constrained zonotope satisfies Assumption 1.

3.2 Inner-approximation of the Pontryagin difference

We are now ready to address the inner-approximation part of Problem 1. First, we recall the following lemma.

Lemma 1. [9, Lemma 2(ii)] *For any set $\mathcal{S}_1, \mathcal{S}_2 \subset \mathbb{R}^n$ and $G \in \mathbb{R}^{m \times n}$ with $m < n$, $G(\mathcal{S}_1 \ominus \mathcal{S}_2) \subseteq (G\mathcal{S}_1) \ominus (G\mathcal{S}_2)$.*

Theorem 1. *Given a non-empty constrained zonotopic minuend $\mathcal{C} = (G_C, c_C, A_C, b_C) \subset \mathbb{R}^n$ and a convex and compact subtrahend $\mathcal{S} \subset \mathbb{R}^n$ that is symmetric about any $c_S \in \mathbb{R}^n$. Let $\Gamma : \mathbb{R}^{N_C \times n}$ solve*

$$\begin{bmatrix} G_C \\ A_C \end{bmatrix} \Gamma = \begin{bmatrix} I_n \\ 0_{M_C \times n} \end{bmatrix}, \quad (18)$$

and $D \in \mathbb{R}^{N_C \times N_C}$ be a diagonal matrix with

$$D_{ii} \triangleq 1 - \rho_{\mathcal{S}_0}(e_i^\top \Gamma), \quad (19)$$

for each $i \in \mathbb{N}_{[1:N_C]}$, where $\mathcal{S}_0 \triangleq \mathcal{S} - c_S$. Then, the constrained zonotope \mathcal{M}^- defined using (16) and D in (19) satisfies (15), provided $D_{ii} \geq 0$ for every $i \in \mathbb{N}_{[1:N_C]}$.

Proof. Given $\mathcal{S}_0 \subset \mathbb{R}^n$, define $\mathcal{V}_0 = \Gamma \mathcal{S}_0 \subset \mathbb{R}^{N_C}$. By definition of Γ , \mathcal{V}_0 satisfies 1) $G_C \mathcal{V}_0 = \mathcal{S}_0 = \mathcal{S} - c_S$, and 2) $A_C \mathcal{V}_0 = \{0_{M_C \times 1}\}$.

Next, define $\mathcal{C}_L \triangleq \mathcal{B}_\infty(A_C, b_C) \ominus \mathcal{V}_0 \subset \mathbb{R}^{N_C}$, and define

$$\mathcal{M}^- \triangleq c_{M^-} + G_C \mathcal{C}_L. \quad (20)$$

with $c_{M^-} \triangleq c_C - c_S$ (see (16)). By Lemma 1 and [23, Thm. 2.1.iv],

$$\begin{aligned} \mathcal{M}^- &\subseteq c_{M^-} + (G_C \mathcal{B}_\infty(A_C, b_C) \ominus (G_C \mathcal{V}_0)) \\ &= c_{M^-} + ((\mathcal{C} - c_C) \ominus (\mathcal{S} - c_S)) \\ &= (c_{M^-} - (c_C - c_S)) + (\mathcal{C} \ominus \mathcal{S}) = \mathcal{C} \ominus \mathcal{S}. \end{aligned} \quad (21)$$

Next, we simplify \mathcal{C}_L as follows,

$$\mathcal{C}_L = \{\xi \mid \forall v \in \mathcal{V}_0, \xi + v \in \mathcal{B}_\infty(A_C, b_C)\} \quad (22)$$

$$= \{\xi \mid \forall v \in \mathcal{V}_0, A_C(\xi + v) = b_C, \|\xi + v\|_\infty \leq 1\} \quad (23)$$

$$= \{\xi \mid A_C \xi = b_C, \forall v \in \mathcal{V}_0, \|\xi + v\|_\infty \leq 1\} \quad (24)$$

$$= \{\xi \mid A_C \xi = b_C\} \cap (\{\xi \mid \|\xi\|_\infty \leq 1\} \ominus \mathcal{V}_0) \quad (25)$$

$$= \{\xi \mid A_C \xi = b_C, \forall i \in \mathbb{N}_{[1:N_C]}, \forall \delta \in \{-1, 1\}, \delta e_i^\top \xi \leq 1 - \rho_{\mathcal{V}_0}(\delta e_i)\} \quad (26)$$

$$= \{\xi \mid A_C \xi = b_C, \forall i \in \mathbb{N}_{[1:N_C]}, |e_i^\top \xi| \leq 1 - \rho_{\mathcal{S}_0}(\Gamma^\top e_i)\} \quad (27)$$

$$= \{\xi \mid A_C \xi = b_C, \forall i \in \mathbb{N}_{[1:N_C]}, |e_i^\top \xi| \leq D_{ii}\} \quad (28)$$

Here, (22) follows from (6d) and the definition of \mathcal{C}_L , (23) follows from (3), (24) follows from the choice of \mathcal{V}_0 , (25) follows from (6d), (26) follows from (8), (27) follows from (4) and from $\rho_{\mathcal{V}_0}(\nu) = \rho_{\mathcal{S}_0}(\Gamma^\top \nu)$ for all $\nu \in \mathbb{R}^{N_C}$ [22, Prop. 2], and from symmetry of \mathcal{S}_0 about the origin implying $\rho_{\mathcal{S}_0}(-\mu) = \rho_{\mathcal{S}_0}(\mu)$ for all $\mu \in \mathbb{R}^n$ by (4), and (28) follows from the definition of D_{ii} (19).

If $D_{ii} < 0$ for any $i \in \mathbb{N}_{[1:N_C]}$, then $\mathcal{C}_L = \emptyset$ by (28), and \mathcal{M}^- defined in (20) is also empty. On the other hand, when $D_{ii} \geq 0$ for all $i \in \mathbb{N}_{[1:N_C]}$, (28) may be expressed as a scaled version of \mathcal{B}_∞ ,

$$\mathcal{C}_L = \{D\xi \mid A_C D\xi = b_C, \|\xi\|_\infty \leq 1\} = D\mathcal{B}_\infty(A_C D, b_C).$$

Thus, $\mathcal{M}^- \subseteq \mathcal{C} \ominus \mathcal{S}$ in (15) using (20) and (21), provided $D_{ii} \geq 0$ for all $i \in \mathbb{N}_{[1:N_C]}$. \square

Theorem 1 inner-approximates the Pontryagin difference (6d) using the support function of the subtrahend \mathcal{S} , without requiring the minuend \mathcal{C} to be full-dimensional (Assumption 1). The condition $D_{ii} \geq 0$ for all $i \in \mathbb{N}_{[1:N_C]}$ in Theorem 1 may be viewed as requiring Γ to additionally satisfy $\Gamma \mathcal{S}_0 \subseteq \{\xi \mid \|\xi\|_\infty \leq 1\}$. Such a choice ensures $\rho_{\mathcal{S}_0}(\Gamma^\top e_i) \leq 1$, and thereby, $D_{ii} \geq 0$ [21, Ex. 3.35(d)].

We now propose a closed-form expression for Γ for full-dimensional minuend \mathcal{C} to address Problem 1.

Theorem 2. *Let Assumption 1 hold for the minuend \mathcal{C} . Then, for any convex and compact subtrahend $\mathcal{S} \subset \mathbb{R}^n$ that is symmetric about any $c_S \in \mathbb{R}^n$, the set \mathcal{M}^- defined in Theorem 1 with $\Gamma = [G_C; A_C]^\dagger [I_n; 0_{M_C \times n}]$ inner-approximates $\mathcal{C} \ominus \mathcal{S}$.*

Proof. Under Assumption 1, $[G_C; A_C]$ has full row rank by Proposition 1. Choose $\Gamma = [G_C; A_C]^\dagger [I_n; 0_{M_C \times n}]$, and observe that Γ satisfies (18), which in turn satisfies the requirements of Theorem 1. \square

Next, we specialize Theorem 2 for some specific types of symmetric sets, as described in Corollary 1 and Table 1.

Corollary 1 (SPECIAL CASES). *Assume the setting of Theorem 2. Then, D in (19) has closed-form expressions for D_{ii} for each $i \in \mathbb{N}_{[1:N_C]}$:*

1) when \mathcal{S} is a convex union of symmetric intervals (1c),

$$D_{ii} = 1 - \|e_i^\top [G_C; A_C]^\dagger [G_S; 0_{M_C \times N_S}]\|_\infty, \quad (29)$$

2) when \mathcal{S} is a zonotope (1d),

$$D_{ii} = 1 - \|e_i^\top [G_C; A_C]^\dagger [G_S; 0_{M_C \times N_S}]\|_1, \quad (30)$$

3) when \mathcal{S} is an ellipsoid (1e),

$$D_{ii} = 1 - \|e_i^\top [G_C; A_C]^\dagger [G_S; 0_{M_C \times N_S}]\|_2. \quad (31)$$

Algorithm 1 Inner-approximation of $\mathcal{C} \ominus \mathcal{S}$

Input: Minuend $\mathcal{C} = (G_C, c_C, A_C, b_C)$ that is full-dimensional and subtrahend \mathcal{S} that is convex, compact, and symmetric about any $c_S \in \mathbb{R}^n$

Output: Constrained zonotope $\mathcal{M}^- \subseteq \mathcal{C} \ominus \mathcal{S}$

```

1:  $\mathcal{S}_0 \leftarrow \mathcal{S} - c_S$ 
2:  $\Gamma \leftarrow [G_C; A_C]^\dagger [I_n; 0_{M_C \times n}]$ 
3:  $D \leftarrow \text{diag}([1 - \rho_{\mathcal{S}_0}(e_1^\top \Gamma); \dots; 1 - \rho_{\mathcal{S}_0}(e_{N_C}^\top \Gamma)])$ 
4: if  $D_{ii} \geq 0, \forall i \in \mathbb{N}_{[1:N_C]}$  then
5:    $\mathcal{M}^- \leftarrow (G_C D, c_C - c_S, A_C D, b_C)$ 
6: else
7:    $\mathcal{M}^- \leftarrow \emptyset$ 
8: end if

```

Proof. Follows from (5) and Theorem 2. □

Corollary 1 lists some broad classes of subtrahends that admits closed-form expressions for the inner-approximation \mathcal{M}^- of the Pontryagin difference $\mathcal{C} \ominus \mathcal{S}$.

Algorithm 1 summarizes the procedure described in Theorems 1 and 2 to inner-approximate $\mathcal{C} \ominus \mathcal{S}$ when the minuend \mathcal{C} is full-dimensional (Assumption 1). For subtrahends that are ellipsoids, zonotopes, or convex unions of symmetric intervals, Step 3 in Algorithm 1 is available in closed form (see Corollary 1), and Algorithm 1 is optimization-free, i.e., it does not require convex optimization solvers.

3.3 Relation of Algorithm 1 with existing two-stage approach for zonotopic subtrahend

For a zonotopic subtrahend \mathcal{S} , we show that the optimization-free Algorithm 1 is closely related to the optimization-based two-stage approach [9] (see Section 2.2). From (1d), $\mathcal{S} = G_S \mathcal{S}_0 + c_S$ where \mathcal{S}_0 is the unit ℓ_∞ -norm ball.

Consider the *matrix least norm* problem [20, Ex. 16.2], which is similar to (9) where the objective is now the Frobenius norm $\|\Gamma\|_F \triangleq \sqrt{\sum_{i=1}^{N_C} \sum_{j=1}^{N_S} \Gamma_{ij}^2}$,

$$\begin{aligned} & \underset{\Gamma \in \mathbb{R}^{N_C \times N_S}}{\text{minimize}} && \|\Gamma\|_F \\ & \text{subject to} && [G_C; A_C]\Gamma = [G_S; 0_{M_C \times N_S}]. \end{aligned} \quad (32)$$

When \mathcal{C} is full-dimensional, the optimal solution of (32) is available in closed-form, $\Gamma^* = [G_C; A_C]^\dagger [G_S; 0_{M_C \times N_S}]$, by Proposition 1 and [20, Ex. 16.2]. Observe that $\Gamma^* = \Gamma G_S$ for Γ prescribed by Theorem 2. Then, we can recover D prescribed by (30) in Corollary 1 using (19) in Theorem 1, where $\rho_{\mathcal{S}_0}(\nu) = \|\nu\|_1$ instead of (5c).

The condition $D_{ii} \geq 0$ is required both in the two-stage approach [9] (see (9)) and in Step 4 of Algorithm 1. Thus, the expression for D_{ii} obtained by Algorithm 1 is identical to that in (10), and Algorithm 1 and [9] differ only in the choice of Γ (or specifically, the choice of objective in (9)) for a zonotopic subtrahend. In other words, Algorithm 1 may be viewed as a generalization of [9] to handle any symmetric, convex, and compact subtrahend. Moreover, thanks to Theorem 2, Algorithm 1 has some computational advantage over [9], as discussed further in Section 6.3.

4 Outer-approximation of Pontryagin difference and sufficient conditions for exactness

In this section, we first address Problem 2, and then use its solution to address the outer-approximation part of Problem 1. We also provide sufficient conditions under which all proposed approximations are exact. We conclude this section with a discussion of implementation considerations for the proposed algorithms.

4.1 Constructing an outer-approximating convex polyhedron for a given constrained zonotope

We address Problem 2 using Algorithm 2 that computes a convex, polyhedral outer-approximation of a constrained zonotope.

Proposition 2. *Given a full-dimensional constrained zonotope \mathcal{C} (Assumption 1), Algorithm 2 computes an convex, polyhedral, outer-approximation of \mathcal{C} in the form of (1a) with at most $2N_C$ linear constraints.*

Algorithm 2 Convex polyhedral outer-approximation of a constrained zonotope \mathcal{C} **Input:** Full-dimensional $\mathcal{C} = (G_C, c_C, A_C, b_C)$ **Output:** Convex polyhedron $\mathcal{P} = \{x : Hx \leq k\} \supseteq \mathcal{C}$ 1: $V \leftarrow [v_1; v_2; \dots; v_{N_C}] \in \mathbb{R}^{N_C \times (n+M_C)}$ with

$$v_i = \frac{e_i^\top [G_C; A_C]^\dagger}{\|e_i^\top [G_C; A_C]^\dagger [G_C; A_C]\|_1}, \quad \forall i \in \mathbb{N}_{[1:N_C]} \quad (33)$$

2: $H \leftarrow [V; -V][I_n; 0_{M_C \times n}]$ 3: $k \leftarrow 1_{(2N_C) \times 1} - [V; -V] \begin{bmatrix} -c_C \\ b_C \end{bmatrix}$ **Algorithm 3** Outer-approximation of $\mathcal{C} \ominus \mathcal{S}$ **Input:** Minuend $\mathcal{C} = (G_C, c_C, A_C, b_C)$ that is full-dimensional and a convex and compact subtrahend \mathcal{S} that is symmetric about any $c_S \in \mathbb{R}^n$ **Output:** Constrained zonotope $\mathcal{M}^+ \supseteq \mathcal{C} \ominus \mathcal{S}$ 1: Compute a convex polyhedron $\mathcal{P} \supseteq \mathcal{C}$ using Algorithm 22: Compute a convex polyhedron $\mathcal{M}_p^+ = \mathcal{P} \ominus \mathcal{S}$ via (8)3: Compute $\mathcal{M}^+ \leftarrow (\mathcal{C} - c_S) \cap \mathcal{M}_p^+$ using (7d)

See Appendix A.2 for the proof of Proposition 2. The key insight used in Proposition 2 is that we can express \mathcal{C} in (1b) as the 1-sublevel set of the optimal value function of a linear program that is always feasible for a full-dimensional \mathcal{C} (see (50) in Appendix A.2). Then, we use strong duality to obtain an outer-approximating convex polyhedron \mathcal{P} , characterized by $2N_C$ feasible solutions (33) to the corresponding dual problem.

While [6, Prop. 3] provides an exact convex polytopic representation of \mathcal{C} using *lifted zonotopes*, it may require a combinatorial number of hyperplanes, and may not be practical for large n and/or N_C . Instead, Algorithm 2 outer-approximates \mathcal{C} with a convex polyhedron \mathcal{P} that has at most $2N_C$ halfspaces, and can be efficiently computed for \mathcal{C} with large n and N_C without relying on convex optimization solvers. Redundant inequalities in \mathcal{P} may be removed via linear programming [4], if desired.

Additional assumptions on \mathcal{C} may be required to ensure that \mathcal{P} is bounded (and, thereby a convex polytope), and representable as a constrained zonotope using [6, Thm. 1]. We provide one such assumption in Section 4.3.

4.2 Outer-approximation of the Pontryagin difference

Next, we address the outer-approximation part of Problem 1. We use Algorithm 2, (8), and (7d) to compute \mathcal{M}^+ , an outer-approximation of the Pontryagin difference $\mathcal{C} \ominus \mathcal{S}$, and summarize the approach in Algorithm 3.

Proposition 3. *For any full-dimensional \mathcal{C} and any convex and compact subtrahend \mathcal{S} that is symmetric about any $c_S \in \mathbb{R}^n$, Algorithm 3 returns $\mathcal{M}^+ \supseteq \mathcal{C} \ominus \mathcal{S}$.*

Proof. By Proposition 2 and (8), \mathcal{M}_p^+ constructed in Step 2 of Algorithm 3 outer-approximates $\mathcal{C} \ominus \mathcal{S}$. Since \mathcal{S} is symmetric about c_S , $(\mathcal{C} - c_S)$ is also an outer-approximation of $\mathcal{C} \ominus \mathcal{S}$ by (6d). We obtain the outer-approximating constrained zonotope \mathcal{M}^+ by intersecting these outer-approximations in Step 3 using (7d). \square

All steps of Algorithm 3 are available in closed-form, when the support function of \mathcal{S} is known in closed-form. Similarly to Algorithm 1, Algorithm 3 is optimization-free, i.e., it does not require convex optimization solvers, for subtrahends that are ellipsoids, zonotopes, or convex unions of symmetric intervals (see (5)).

4.3 Sufficient conditions for exactness

Now, we state a sufficient condition under which the approximations of the Pontryagin difference computed by Algorithms 1 and 3, and the convex polyhedral outer-approximation of a constrained zonotope computed by Algorithm 2 are exact.

Assumption 2. *The minuend \mathcal{C} has a MINROW representation (1b) such that $n + M_C = N_C$.*

When Assumption 2 holds, $[G_C; A_C]$ is square and invertible by Proposition 1, since Assumption 2 implies Assumption 1.

Proposition 4. (SUFFICIENT CONDITIONS FOR EXACTNESS OF POLYHEDRAL COVER) *Under Assumption 2, Algorithm 2 computes a convex polytope $\mathcal{P} = \mathcal{C}$.*

Proposition 5. (SUFFICIENT CONDITIONS FOR EXACTNESS OF PONTRYAGIN DIFFERENCE) *Under Assumption 2, the approximations \mathcal{M}^- and \mathcal{M}^+ computed using Algorithms 1 and 3 satisfy $\mathcal{M}^- = \mathcal{M} = \mathcal{C} \ominus \mathcal{S} = \mathcal{M}^+$.*

See Appendices A.3 and A.4 for the proofs. Under Assumption 2, \mathcal{M}_p^+ computed in Step 2 of Algorithm 3 is $\mathcal{C} \ominus \mathcal{S}$ by Proposition 4. Consequently, we can skip Step 3 of Algorithm 3, and directly compute a constrained zonotope representation of \mathcal{M} from the convex polytope \mathcal{M}_p^+ .

Algorithm 1, 3 together address Problem 1, as shown by Theorems 1, 2, and Propositions 3, 5. Algorithm 2 addresses Problem 2, as shown by Propositions 2 and 4.

4.4 Implementation considerations

The use of pseudoinverse $[G_C; A_C]^\dagger$ in Algorithms 1, 2, and 3 was motivated by providing closed-form expressions for D_{ii} (19) and v_i (33). However, the computation of $[G_C; A_C]^\dagger$ can be computationally expensive for large N_C and M_C . In practice, it suffices to compute a minimum norm solution of systems of linear equations — a solution Γ in (18) for Step 2 of Algorithm 1, a solution ξ to $A_C \xi = b_C$ in Step 4 of Algorithm 1, and a solution V^\top to $[G_C; A_C]^\top V^\top = I_{N_C}$ for Step 1 of Algorithm 2 (where $V[G_C; A_C]$ is later normalized row-wise in ℓ_1 -norm).

We can also compute a minimum norm solution without computing the pseudoinverse explicitly via QR factorization or complete orthogonal decomposition [20, Ch. 12]. Existing algorithms can also exploit sparsity [20, Ch. 12.3]. In Sections 6 and 7, our MATLAB implementation of Algorithms 1, 2, and 3 utilizes `lsqminnorm` to compute minimum norm solutions and uses sparse matrices for computational efficiency.

5 Inner-approximation of robust controllable sets

We now address Problem 3 by inner-approximating the T -step RC set using Algorithm 1 and the set recursion (14). We consider both cases described in Problem 3, characterize the representation complexity of the computed inner-approximations, and show that their representation complexities grow linearly with T .

Throughout this section, we will assume that the input set \mathcal{U}_t and the goal set \mathcal{G} are convex polytopes, hence, representable as constrained zonotopes, and the additive disturbance set \mathcal{W}_t is a convex and compact set that is symmetric about any $c_W \in \mathbb{R}^p$.

5.1 Convex polyhedral \mathcal{X}_t and invertible A_t

Given a finite horizon $T \in \mathbb{N}$, we consider the case where A_t matrices of the linear system (13) are invertible, and state constraints \mathcal{X}_t are polyhedra for all $t \in \mathbb{N}_{[0:T-1]}$. Since \mathcal{X}_t can be unbounded, they may not be representable as constrained zonotopes. However, we can still inner-approximate the RC sets as constrained zonotopes using (7d), as shown in this section.

For all $t \in \mathbb{N}_{[0:T-1]}$, we break down the set recursion (14) to compute the T -step RC set into four steps:

$$\mathcal{K}_{t,\text{inner}}^{\text{interim},1} \subseteq \mathcal{K}_t^{\text{interim},1} = \mathcal{K}_{t+1} \ominus F_t \mathcal{W}_t, \quad (34a)$$

$$\mathcal{K}_t^{\text{interim},2} = \mathcal{K}_{t,\text{inner}}^{\text{interim},1} \oplus (-B_t \mathcal{U}_t), \quad (34b)$$

$$\mathcal{K}_t^{\text{interim},3} = A_t^{-1} \mathcal{K}_t^{\text{interim},2}, \quad (34c)$$

$$\mathcal{K}_t = \mathcal{K}_t^{\text{interim},3} \cap \mathcal{X}_t. \quad (34d)$$

The recursion (34) is initialized with a constrained zonotope $\mathcal{K}_T = \mathcal{G}$. We use Theorem 2 to compute a constrained zonotope $\mathcal{K}_{t,\text{inner}}^{\text{interim},1}$ in (34a). Then, we compute (34b)–(34d) exactly using (7). Thus, for all $t \in \mathbb{N}_{[0:T-1]}$, the sets \mathcal{K}_t , $\mathcal{K}_{t,\text{inner}}^{\text{interim},1}$, $\mathcal{K}_t^{\text{interim},2}$, and $\mathcal{K}_t^{\text{interim},3}$ are constrained zonotopes, and $\mathcal{K}^- = \mathcal{K}_0$ is an inner-approximation of the T -step RC set.

Table 2 describes the representation complexity of various constrained zonotopes involved at each step of (34). For ease of discussion, we assume that \mathcal{X}_t , \mathcal{U}_t , and \mathcal{W}_t are time-invariant, i.e., $\mathcal{X}_t = \mathcal{X}$, $\mathcal{U}_t = \mathcal{U}$, and $\mathcal{W}_t = \mathcal{W}$, for all $t \in \mathbb{N}_{[0:T]}$. Additionally, we assume that \mathcal{X} is characterized by N_X hyperplanes. Given representation complexities

| Set \mathcal{S} | Eq. no. | $N_{\mathcal{S}}$ | $M_{\mathcal{S}}$ |
|---|---------|-------------------------|-------------------------|
| $\mathcal{K}_{t,\text{inner}}^{\text{interim},1}$ | (34a) | $N_{K,t+1}$ | $M_{K,t+1}$ |
| $\mathcal{K}_t^{\text{interim},2}$ | (34b) | $N_{K,t+1} + N_U$ | $M_{K,t+1} + M_U$ |
| $\mathcal{K}_t^{\text{interim},3}$ | (34c) | $N_{K,t+1} + N_U$ | $M_{K,t+1} + M_U$ |
| \mathcal{K}_t | (34d) | $N_{K,t+1} + N_U + N_X$ | $M_{K,t+1} + M_U + N_X$ |

Table 2: Representation complexity (see Definition 1) for various sets involved in computing an inner-approximation to the T -step RC set using (34), where $\mathcal{C}(\mathcal{K}_{t+1}) = (n, N_{K,t+1}, M_{K,t+1})$ and $\mathcal{C}(\mathcal{U}) = (m, N_U, M_U)$, and \mathcal{X} is characterized by N_X hyperplanes. Observe that the representation complexity grows by $(0, N_U + N_X, M_U + N_X)$ with each step of the recursion.

$\mathcal{C}(\mathcal{K}_{t+1}) = (n, N_{K,t+1}, M_{K,t+1})$ and $\mathcal{C}(\mathcal{U}) = (m, N_U, M_U)$, the rows of Table 2 follow from Theorem 2, (7b), (7a), and (7d), respectively.

With $\mathcal{C}(\mathcal{G}) = (n, N_G, M_G)$, the representation complexity of the inner-approximation of the T -step RC set is

$$\mathcal{C}(\mathcal{K}^-) = (n, N_G + T(N_U + N_X), M_G + T(M_U + N_X)). \quad (35)$$

Observe that the representation complexity of \mathcal{K}^- does not depend on the disturbance set \mathcal{W} , due to Theorem 2, and grows linearly with T .

5.2 Convex polytopic \mathcal{X}_t

We now consider the case where the state constraints \mathcal{X}_t are convex polytopes for all $t \in \mathbb{N}$, and are representable using constrained zonotopes. Unlike Section 5.1, we no longer assume that A_t is invertible.

Similarly to (34), we separate the set recursion (14) into *three* steps performed for all $t \in \mathbb{N}_{[0:T-1]}$:

$$\mathcal{K}_{t,\text{inner}}^{\text{interim},1} \subseteq \mathcal{K}_t^{\text{interim},1} = \mathcal{K}_{t+1} \ominus F_t \mathcal{W}_t, \quad (36a)$$

$$\mathcal{K}_t^{\text{interim},2} = \mathcal{K}_{t,\text{inner}}^{\text{interim},1} \oplus (-B_t \mathcal{U}_t), \quad (36b)$$

$$\mathcal{K}_t = \mathcal{X}_t \cap_{A_t} \mathcal{K}_t^{\text{interim},2}, \quad (36c)$$

where (36c) combines (34c) and (34d) into a single step using (7c). Given representation complexities $\mathcal{C}(\mathcal{X}) = (n, N_X, M_X)$ and $\mathcal{C}(\mathcal{U}) = (m, N_U, M_U)$, the representation complexity of \mathcal{K}_t grows by $(0, N_U + N_X, M_U + M_X + n)$ at each step of the set recursion (see (7c) and Table 2). Consequently, for \mathcal{G} with $\mathcal{C}(\mathcal{G}) = (n, N_G, M_G)$, the set representation complexity of the inner-approximation of the T -step RC step is

$$\mathcal{C}(\mathcal{K}^-) = (n, N_G + T(N_U + N_X), M_G + T(M_U + M_X + n)). \quad (37)$$

Similarly to Section 5.1, the representation complexity of \mathcal{K}^- in (37) also grows linearly with T and does not depend on the disturbance set \mathcal{W} .

Remark 1. We can also use the set recursions discussed in Section 5.1 and 5.2 in conjunction with Algorithm 3 to obtain an outer-approximation to the T -step RC set.

Remark 2. In this work, we did not use the exact or approximate reduction techniques [6, 7, 25] that may lower the representation complexity at the expense of additional computation or accuracy or both. On the other hand, it is straightforward to apply these results to the sets computed in this work for a further reduction in the set representation complexity.

6 Case studies

We now demonstrate the computational efficiency, scalability, and utility of our approach in several case studies. First we consider two case studies involving low-dimensional systems to illustrate the advantage of the proposed approach in computing time when compared to existing inner-approximating approaches based on constrained zonotopes [9], and exact approaches based on polyhedra [4]. Then, we discuss the scalability of the approach by computing the RC set for a chain of mass-spring-damper system, and empirically demonstrate that the proposed approach is numerically stable and can compute the RC sets for high dimensional systems and long horizons.

We perform the presented computations in a standard computer with Intel CPU i9-12900KF processor (3.2 GHz, 16 cores) and 64 GB RAM, running MATLAB 2022b. We use YALMIP [26] to set up the optimization problems

| Property | Exact RC set [4] | \mathcal{W} represented as an ellipsoid | | Zonotopic $\mathcal{W}^+ \supset \mathcal{W}$ | |
|--|---------------------|---|--------------------------|---|---------------|
| | | Proposed \mathcal{M}^- | Proposed \mathcal{M}^+ | Proposed \mathcal{M}^- | Two-stage [9] |
| True \mathcal{W} is a ball (left) | | | | | |
| Ratio of area | 1 | 0.97 | 1.67 | 0.70 | 0.67 |
| Compute time (s) | 2.044 | 0.012 | 4.064 | 0.010 | 1.594 |
| Ratio of time | 177.39 | 1 | 352.66 | 0.86 | 138.29 |
| True \mathcal{W} is an ellipsoid (right) | | | | | |
| Ratio of area | 1 | 0.77 | 3.46 | 0.37 | 0.22 |
| Compute time (s) | 2.958 | 0.017 | 4.199 | 0.014 | 1.520 |
| Ratio of time | 176.65 | 1 | 250.78 | 0.84 | 90.78 |

Table 3: Comparison of various approaches for Example 6.1. The proposed approach is about two orders of magnitude faster than existing approaches [4, 9], while producing sufficiently accurate approximations.

with MOSEK [27] and GUROBI [28] as solvers. For two-dimensional plots of constrained zonotopes \mathcal{C} , we compute the appropriate convex polytopic approximations via support function and support vector computations (4) in 100 equi-spaced directions in \mathbb{R}^2 . We estimate the volume of the sets via sampling.

6.1 Double integrator example with convex polytopic \mathcal{X}

We consider the computation of RC set for a double integrator system with convex polytopic state constraints \mathcal{X} and an ellipsoidal disturbance set \mathcal{W} . The linear time-invariant system matrices are

$$A = \begin{bmatrix} 1 & \Delta T \\ 0 & 1 \end{bmatrix}, \quad B = \begin{bmatrix} (\Delta T)^2/2 \\ \Delta T \end{bmatrix}, \quad \text{and } F = I_2,$$

with the sampling period $\Delta T = 0.1$, the input set $\mathcal{U} = [-2, 2]$ that is an interval, the disturbance set $\mathcal{W} = (0.1I_2, [0; 0])$ or $\mathcal{W} = \text{diag}([0.2, 0.04], [0.1; 0.1])$ that is a circle or an ellipsoid respectively, and the state constraints $\mathcal{X} = \mathcal{G} = [-2, 2] \times [-3, 3]$ that are time-invariant, axis-aligned rectangles.

We generate inner-approximations of the T -step RC set using the recursion in Section 5.2 for $T = 20$ with an exact ellipsoidal representation of \mathcal{W} and a zonotopic outer-approximation $\mathcal{W}^+ = (G_W, c_W) \supset \mathcal{W}$ where the Pontryagin difference is inner-approximated using Algorithm 1. We also compare the computed sets with the exact sets computed using MPT3 where the vertex-facet enumeration was accomplished using Fourier-Motzkin elimination [4], and the inner-approximations of the RC sets using the two-stage approach with the zonotopic \mathcal{W}^+ [9]. We also compute an outer-approximation of the RC sets using Algorithm 3, as discussed in Remark 1.

Table 3 shows that the proposed inner-approximation approach with ellipsoidal \mathcal{W} is about two orders of magnitude faster than the exact approach [4] and the two-stage approach [9], while providing reasonably accurate inner-approximations (about 97% and 77% of the area of the exact RC set in the first and second case respectively). The proposed inner-approximation approach with zonotopic \mathcal{W}^+ is slightly faster than with ellipsoidal \mathcal{W} , but is more conservative due to the zonotopic outer-approximation of the disturbance set. The shorter computation times of the proposed approach are a direct result of Theorems 1 and 2, since the implementation of the set recursion in Section 5.2 can be accomplished in closed-form, i.e., optimization-free. The proposed outer-approximation approach is slower than the inner-approximation approach, primarily due to the use of linear programming to produce a minimal representation of the convex polyhedron in Step 1 of Algorithm 3 to manage the representation complexity. For most safe constrained control problems, an inner-approximation of the T -step RC set is sufficient.

Figure 1 shows that the RC sets and their corresponding inner-approximations, associated with a ball-shaped \mathcal{W} (left) and an ellipsoidal \mathcal{W} (right). As expected, the inner-approximations of the RC set constructed using zonotopic \mathcal{W}^+ are more conservative than their ellipsoid-based counterparts in both cases. On the other hand, the proposed inner-approximations with zonotopic \mathcal{W}^+ are identical (left) or similar (right) to the inner-approximations produced by the existing two-stage approach [9], while requiring significantly shorter computation time (see Table 3).

6.2 An example with convex polyhedral \mathcal{X}

We now consider the computation of RC set over a long horizon $T = 100$, similar to [9, Ex. 2]. Consider a stable, discrete-time, linear time-invariant system with matrices

$$A = \begin{bmatrix} 0.99 & 0.02 \\ -0.15 & 0.99 \end{bmatrix}, \quad B = \begin{bmatrix} -0.01 \\ 0.08 \end{bmatrix}, \quad \text{and } F = I_2,$$

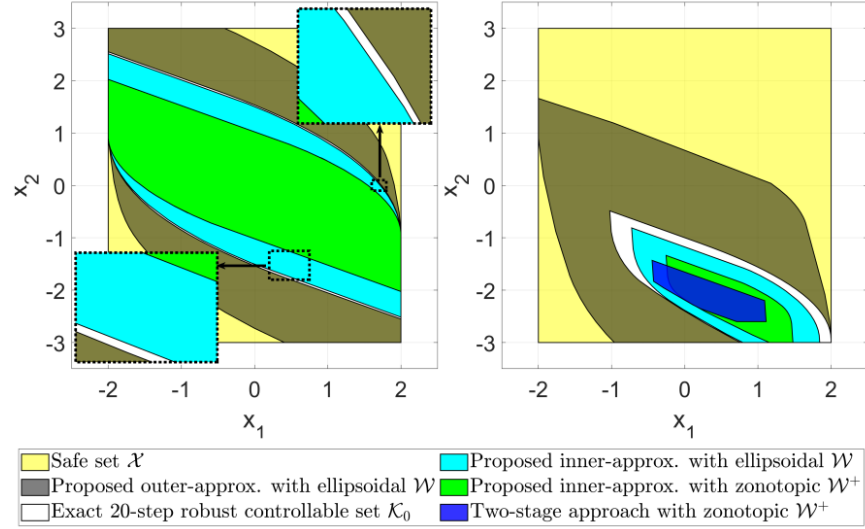


Figure 1: Robust controllable set for a double integrator system over a horizon of $T = 20$ for a ball-shaped \mathcal{W} (left) and an ellipsoidal \mathcal{W} (right) computed via existing approaches (exact [4] and two-stage approach [9]) and the proposed approximations computed using the recursion in Section 5.2. The insets in the left figure show that the proposed approach with ellipsoidal \mathcal{W} (cyan) provides sufficiently accurate inner-approximations of the exact RC set (white).

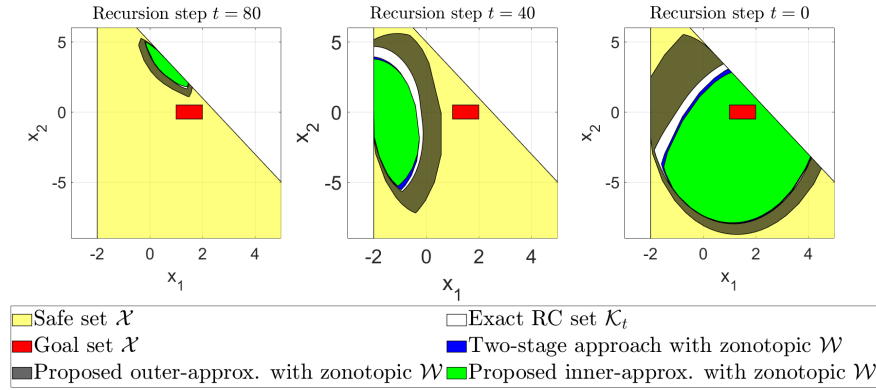


Figure 2: Snapshots of the 100-step robust controllable sets from various methods for recursion steps $t \in \{0, 40, 80\}$ (see (34d) in Section 5.1). Our approach computes inner-approximations of the RC set that are similar to those obtained using the exact approach [4] and the two-stage approach [9], with significantly lower computational effort (see Table 4).

and an interval input set $\mathcal{U} = [-1.5, 1.5]$, zonotopic disturbance set $\mathcal{W} = (0.01I_2, [0; 0])$, zonotopic goal set $\mathcal{G} = (0.5I_2, [1.5; 0])$, and convex polyhedral, time-invariant state constraints $\mathcal{X} = \{x | [-1, 0; 2, 1]x \leq [2; 5]\}$.

Since the state constraints are polyhedral and A is invertible, we generate inner-approximations of the T -step RC set using the recursion in Section 5.1. Similarly to Section 6.1, we compare the obtained sets with their exact counterparts computed using MPT3 [4] and the inner-approximations obtained using the two-stage approach [9]. We also compute an outer-approximation of the RC sets using Algorithm 3.

Table 4 shows that the proposed inner-approximating approach with zonotopic \mathcal{W} is over two to three orders of magnitude faster than the existing approaches [4, 9], while providing reasonably accurate inner-approximations that cover about 89% of the area of the exact RC set, as in Section 6.1. The shorter computation time compared to existing approaches is attributed to the optimization-free implementation of Section 5.1, by Theorem 2 and Corollary 1.

Figure 2 shows the 100-step RC sets computed by various methods at recursion step $t \in \{0, 40, 80\}$. Unlike in Section 6.1, the proposed inner-approximation of the RC set in this case is contained in the inner-approximation

| Property | Exact RC set [4] | \mathcal{W} represented as a zonotope | | |
|------------------|---------------------|---|--------------------------|---------------|
| | | Proposed \mathcal{M}^- | Proposed \mathcal{M}^+ | Two-stage [9] |
| Ratio of area | 1 | 0.89 | 1.36 | 0.92 |
| Compute time (s) | 110.661 | 0.090 | 158.753 | 10.192 |
| Ratio of time | 1235.87 | 1 | 1772.96 | 113.82 |

Table 4: Comparison of various approaches for Example 6.2. The proposed approach is over two to three orders of magnitude faster than existing approaches [4,9], while producing sufficiently accurate approximations, even for a long horizon of $T = 100$ time steps.

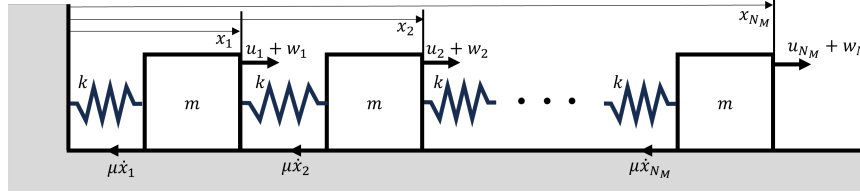


Figure 3: Chain of N_M mass-spring-damper systems.

using the two-stage approach [9]. However, the conservativeness of the proposed approach compared to the two-stage approach [9] appears minimal, covering about 89% vs 92% of the area of the exact RC set.

6.3 Scalability: Chain of damped spring-mass systems

We now demonstrate scalability of the representation complexity for the proposed inner-approximation. Specifically, we compute the RC set of a chain of $N_M \in \mathbb{N}$ homogenous mass-spring-damper systems, see Figure 3, for a range of chain lengths, i.e., different system dimension, and set recursion lengths, i.e., different horizon T . The chain system has the following continuous-time linear time-invariant dynamics,

$$\ddot{x}_1 = -\frac{2k}{m}x_1 + \frac{k}{m}x_2 - \frac{\mu}{m}\dot{x}_1 + w_1 + u_1, \quad (38a)$$

$$\ddot{x}_{N_M} = -\frac{2k}{m}x_{N_M} + \frac{k}{m}x_{(N_M-1)} - \frac{\mu}{m}\dot{x}_{N_M} + w_{N_M} + u_{N_M}, \quad (38b)$$

$$\ddot{x}_j = -\frac{2k}{m}x_j + \frac{k}{m}(x_{j-1} + x_{j+1}) - \frac{\mu}{m}\dot{x}_j + w_j + u_j, \quad (38c)$$

where $j \in \mathbb{N}_{[2:(N_M-1)]}$. The system (38) describes a $(2N_M)$ -dimensional system parameterized by the spring constant k , the mass m , and the friction coefficient μ . Additionally, each spring is actuated by an acceleration input $u_i \in \mathcal{U} \subset \mathbb{R}$ and is subject to an acceleration disturbance $w \in \mathcal{W} \subset \mathbb{R}$.

After discretizing (38) with sampling time $\Delta T = 0.1$ using zero-order hold, we consider the following computations of T -step RC sets:

- 1) $n \in \mathbb{N}_{[4:100]}$ with $T = 20$ using Section 5.2,
- 2) $n \in \mathbb{N}_{[4:100]}$ with $T = 40$ using Section 5.2,
- 3) $n \in \mathbb{N}_{[4:50]}$ with $T = 20$ using two-stage approach [9],
- 4) $n \in \mathbb{N}_{[4:14]}$ with $T = 20$ using exact approach [4].

We use parameters $k = 0.1$, $m = 0.1$, and $\mu = 0.01$, input set $\mathcal{U} = \llbracket -0.1, 0.1 \rrbracket^{N_M}$, disturbance set $\mathcal{W} = \llbracket -0.0001, 0.0001 \rrbracket^{N_M}$, and state constraints $\mathcal{X} = \mathcal{G} = (\llbracket -0.2, 0.2 \rrbracket \times \llbracket -0.5, 0.5 \rrbracket)^{N_M}$.

Figure 4 shows that the proposed method takes significantly shorter computation time to produce an inner-approximation to the 20-step RC sets, when compared to existing methods [4,9]. Specifically, we observe that our approach takes 12.52 seconds to inner-approximate the 20-step RC set for a 100-dimensional system ($N_M = 50$). On the other hand, the two-stage approach [9] took 649.74 seconds (about 10 minutes) to compute an inner-approximation for the 20-step RC set for much smaller dimensional system $n = 40$ ($N_M = 20$). We encountered numerical issues for the exact set computation using MPT3 [4] beyond $n = 14$ ($N_M = 7$). As expected, the proposed approach took longer to compute the RC sets for an horizon $T = 40$ compared to the sets for an horizon $T = 20$, but still computed an inner-approximation to the 40-step RC set for the 100 dimensional system in 126.53 seconds (about 2 minutes). The scalability of the proposed approach compared to existing approaches may be attributed to the optimization-free implementation of Section 5.2, made possible by Theorem 2 and Corollary 1.

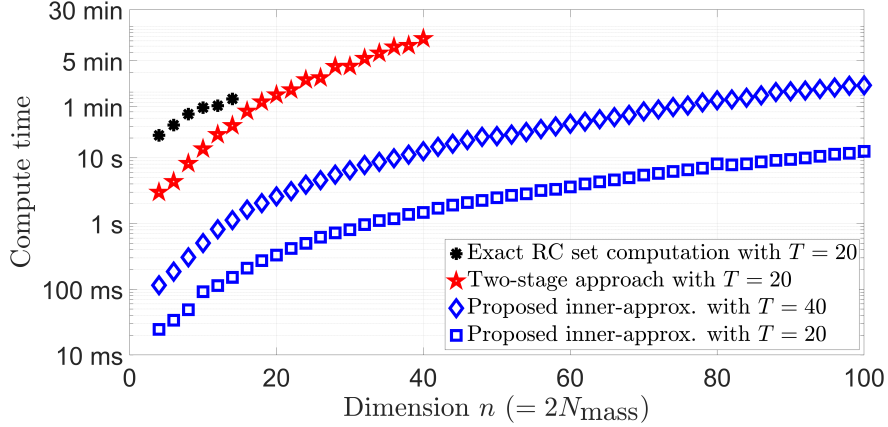


Figure 4: Time taken by various methods to compute the RC sets for varying system dimension n . The proposed method takes 12.52 seconds to inner-approximate 20-step RC sets for a 100-dimensional system. In contrast, existing methods (the exact computation using MPT3 [4] and the two-stage approach in [9]) require longer computation time to tackle lower dimensional systems. We also report the time taken by the proposed method to inner-approximate 40-step RC sets.

We also note that the representation complexity of the proposed inner-approximations grows moderately. For a 10-dimensional system, an inner-approximating constrained zonotope \mathcal{K} for the 20-step RC set had a representation complexity of $\mathcal{C}(\mathcal{K}) = (10, 730, 620)$. As noted in Remark 2, one could use exact or approximate reduction techniques (see [6, 7, 25]) to further lower the set representation complexities, if so desired.

7 Application: Abort-safe rendezvous

Abort safety in spacecraft rendezvous [11, 13, 29] requires that a spacecraft in nominal operation approaches a target while retaining the ability to avoid collision with the target in the event of an anomaly or a failure. In [11], we showed that the problem of abort-safe spacecraft rendezvous could be encoded using RC sets, and we computed these sets using polytopes. However, such an approach is unreliable in high-dimensions and suffers from numerical issues, which motivates the computation of the RC sets using constrained zonotopes. Additionally, in order to guarantee safety, we require an exact computation or inner-approximation of the RC sets.

In this work, we consider rendezvous to a future Lunar gateway flying in a near-rectilinear halo orbit (NRHO) around the Moon [18]. To minimize the use of fuel, we allow the spacecraft to utilize all 3 degrees of freedom in its approach. We compute six-dimensional RC sets that constrain the rendezvous trajectory in order to guarantee that, in the event of an anomaly, off-nominal operation of the spacecraft allows for a safe abort maneuver. Additionally, the trajectory must lie in a line-of-sight cone that arises from sensing and communication requirements, and is determined to ensure that the Sun stays behind the spacecraft, maximizing the perceptibility of the Lunar gateway.

Nominal dynamics: We obtain the unactuated nonlinear dynamics of the spacecraft in the vicinity of the Lunar gateway by considering Earth and Moon’s gravitational forces and dominant perturbations [30]. We linearize the dynamics around the NRHO of the gateway, and discretize the dynamics in T_{sample} -long time intervals to obtain the relative dynamics [29],

$$x_{t+1} = A_t x_t + B_t u_t, \quad (39)$$

with state (position and velocity) $x_t \in \mathbb{R}^6$, input $u_t \in \mathcal{U} \subset \mathbb{R}^3$, B_t as the last three columns of A_t , and perfect state measurements. In (39), the input u_t corresponds to impulsive changes in velocities.

Off-nominal dynamics: We consider three modifications to the nominal dynamics in the event of failure — limited actuation to model the event where the main thrusters fail and the spacecraft is forced to use redundant thrusters like attitude thrusters, process noise to model the resulting actuation uncertainty, and measurement noise to model sensing uncertainty that may increase with the use of redundant thrusters. The need for redundant thrusters is well-known in space applications to ensure safety in off-nominal scenarios [31]. We assume that the process and measurement noises are drawn from pre-determined bounded sets that may be characterized via offline statistical analysis [31].

Specifically, the off-nominal dynamics after a failure event at time t are,

$$z_{k+1|t} = A_t z_{k|t} + B_t(u_{k|t} + w_{k|t}), \quad (40a)$$

$$\hat{z}_{k|t} = z_{k|t} + \eta_{k|t}, \quad (40b)$$

where $z_{k|t}$ is the state after failure at time $k \geq t$, the failure trajectory is initialized by $z_{t|t} = x_t$ the nominal state at failure time t , and $w_{k|t} \in \mathcal{W}_{\text{off-nom}} \subset \mathbb{R}^3$ and $\eta_{k|t} \in \mathcal{E}_{\text{off-nom}} \subset \mathbb{R}^6$ are bounded disturbances to the input and post-failure state respectively. The bounded disturbances model the actuation mismatch and sensing limitations that can become prominent after failure. Additionally, the post-failure input $u_t \in \mathcal{U}_{\text{off-nom}} \subset \mathcal{U}$, where $\mathcal{U}_{\text{off-nom}}$ encodes the limited actuation available after failure. Since we have access to only imperfect measurements post-failure, we consider a feedback controller $\pi : \mathbb{R}^6 \rightarrow \mathcal{U}_{\text{off-nom}}$ that provides a post-failure control u in (40) given the current state estimate $\hat{z} \in \mathbb{R}^6$. Let Π be the set of all such feedback controllers.

From (40), the state estimate \hat{z}_t follows the dynamics,

$$\hat{z}_{t+1} = A_t \hat{z}_t + B_t u_t + \phi_t, \quad (41)$$

with disturbance $\phi_t \in \Phi_t = \mathcal{E}_{\text{off-nom}} \oplus (B_t \mathcal{W}_{\text{off-nom}}) \oplus (-A_t \mathcal{E}_{\text{off-nom}})$. From (40b), the post-failure true state z_t and corresponding state estimate \hat{z}_t satisfy

$$z_t \in \hat{z}_t + (-\mathcal{E}_{\text{off-nom}}) \text{ and } \hat{z}_t \in z_t + \mathcal{E}_{\text{off-nom}}. \quad (42)$$

Rendezvous constraints: We consider the problem of navigating the spacecraft to a target set $\mathcal{T} \subset \mathbb{R}^3$ in front of the Lunar gateway. The designed nominal rendezvous must lie inside a line-of-sight cone $\mathcal{L} \subset \mathbb{R}^3$ originating from the Lunar gateway, and the trajectory must stay outside a keep-out set $\mathcal{D} \subset \mathbb{R}^3$ around the Lunar gateway during the rendezvous maneuver. Additionally, for some pre-determined post-failure safety horizon $T_{\text{safe}} \in \mathbb{N}$, at any time t , the nominal state x_t must satisfy the abort-safety requirement:

$$\text{(Abort-safety): } \begin{cases} \forall k \in \mathbb{N}_{[t:t+T_{\text{safe}}]}, \exists \pi_k \in \Pi, \forall w_{k|t} \in \mathcal{W}_{\text{off-nom}}, \forall \eta_{k|t} \in \mathcal{E}_{\text{off-nom}}, \\ z_{k|t} \text{ in (40) with } u_{k|t} = \pi_k(\hat{z}_{k|t}) \text{ satisfies } z_{k|t} \notin \mathcal{D}, \text{ given } z_{t|t} = x_t. \end{cases} \quad (43)$$

Informally, (43) requires the nominal trajectory to permit steering the spacecraft to continue staying outside \mathcal{D} using limited actuation and imperfect state information under perturbed dynamics (40) over a safety horizon of length T_{safe} , in the event of a failure at time t .

Optimal control problem: Given initial state x_0 , the optimal control problem is formulated as,

$$\begin{aligned} \min \quad & \sum_t (\text{dist}(x_t, \mathcal{T})^2 + \lambda \|u_t\|_2) \\ \text{s. t.} \quad & \text{Nominal dynamics (39) from } x_0, \\ & \forall t, \quad x_t \in \mathcal{L}, \text{ and } x_t \notin \mathcal{D} \\ & \forall t, \quad x_t \text{ meets abort-safety requirement (43).} \end{aligned} \quad (44)$$

For $\lambda > 0$, the objective of (44) balances the typical goals of rendezvous — approaching the target set \mathcal{T} while limiting the energy spent. We measure the energy spent in rendezvous [13] as $(\Delta v)_t = \|u_t\|_2$.

Enforcement of (Abort-safety) using RC sets: Similarly to [11], we encode the abort-safety requirements using appropriately defined RC sets. Using (41) and (42), we derive a sufficient condition for (43) based on RC sets. Let $\mathcal{S}^c = \mathbb{R}^3 \setminus \mathcal{S}$ be the complement of a set $\mathcal{S} \subseteq \mathbb{R}^3$.

Proposition 6. (SUFFICIENT CONDITION FOR ABORT-SAFETY) *Consider a polytopic keep-out set $\mathcal{D} = \bigcap_{i=1}^{N_D} \mathcal{H}_i$ for any appropriately defined N_D halfspaces $\mathcal{H}_i \subset \mathbb{R}^3$, and $\mathcal{E}_{\text{off-nom}}$ that is symmetric about the origin. Let $\mathcal{K}(s, T_{\text{safe}}, \mathcal{H}_i^c \ominus \mathcal{E}_{\text{off-nom}})$ denote the T_{safe} -step RC set for dynamics (41) characterized by $\{(A_t, B_t, \Phi_t)\}_{t=s}^{s+T_{\text{safe}}}$, input set $\mathcal{U}_{\text{off-nom}}$, and time-invariant state constraints $\mathcal{X}_t = \mathcal{G} = \mathcal{H}_i^c \ominus \mathcal{E}_{\text{off-nom}}$. At any time $s \in \mathbb{N}$ such that $x_s \in \bigcup_{i=1}^{N_D} \left(\mathcal{K}(s, T_{\text{safe}}, \mathcal{H}_i^c \ominus \mathcal{E}_{\text{off-nom}}) \ominus \mathcal{E}_{\text{off-nom}} \right)$, then x_s satisfies (43).*

See Appendix A.5 for the proof. Motivated by Proposition 6, we solve the optimal control problem (44) using a receding horizon framework for tractability.

For a finite planning horizon $T_{\text{plan}} \in \mathbb{N}$, consider the following (non-convex) optimization problem that approximates (44),

$$\begin{aligned}
& \underset{\substack{x_{(t+1)|t}, \dots, x_{(t+T_{\text{plan}})|t} \\ u_{t|t}, \dots, u_{(T_{\text{plan}}-1)|t}}}{\text{minimize}} & \sum_t (\text{dist}(x_t, \mathcal{T})^2 + \lambda \|u_t\|_2) \\
& \text{subject to} & \text{Dynamics (39) defines } x_{k|t} \text{ for } k \in \mathbb{N}_{[t+1:t+T_{\text{plan}}]}, \text{ given } x_t, \\
& \forall k \in \mathbb{N}_{[t+1:t+T_{\text{plan}}]}, & x_{k|t} \in \mathcal{L}, \quad x_{k|t} \in \bigcup_{i=1}^{N_D} \mathcal{H}_i^{\mathcal{C}}, \quad u_{k-1|t} \in \mathcal{U} \\
& \forall k \in \mathbb{N}_{[t+1:t+T_{\text{plan}}]}, & x_{k|t} \in \bigcup_{i=1}^{N_D} \mathcal{K}'_i(k, k + T_{\text{safe}}),
\end{aligned} \tag{45}$$

where $\mathcal{K}'_i(k, k + T_{\text{safe}}) = \mathcal{K}(k, k + T_{\text{safe}}, \mathcal{H}_i^{\mathcal{C}} \ominus \mathcal{E}_{\text{off-nom}}) \ominus \mathcal{E}_{\text{off-nom}}$. The optimization problem (45) is non-convex due to *disjunctive constraints* [32].

For a sampling time $T_{\text{sample}} = 20$ minutes, we solve (44) using a receding horizon framework with a planning horizon of 2 hours ($T_{\text{plan}} = 6$) and an abort-safety time horizon of 6 hours ($T_{\text{safe}} = 18$). We consider an impulse-based control with the nominal control set $\mathcal{U} = [-1/3, 1/3]$ (in m/s), off-nominal input set $\mathcal{U}_{\text{off-nom}} = 0.1\mathcal{U}$, post-failure process noise in the ellipsoid $\mathcal{W}_{\text{off-nom}} = (1/60I_3, 0_{3 \times 1})$ (in m/s), and post-failure measurement noise in the ellipsoid $\mathcal{E}_{\text{off-nom}} = (\text{diag}(1, 1, 1, 1/60, 1/60, 1/60), 0_{6 \times 1})$ (in m and m/s). We define the origin-centered keep-out set $\mathcal{D} = [-100, 100]^3$ (in m) which contains the Lunar gateway [18]. We also define a proper cone characterized by four rays originating from the origin as the “line-of-sight cone” $\mathcal{L} = \{x \in \mathbb{R}^3 | [0, 1, -1; 0, 1, 1; -1, 1, 0; 1, 1, 0]x \leq 0_{4 \times 1}\}$ for ease of discussion. We define an ellipsoidal target set $\mathcal{T} = (0.05I_3, c_{\text{target}})$ with $c_{\text{target}} = [0.2416; -0.4017; -0.1738]$ and initial state $x_0 = [1.4498; -2.4105; -1.0429; 0.01; 0.01; 0.01]$ such that the target is 0.5 km and the initial state is 3 km away from the origin with non-zero initial velocity. We rotate \mathcal{D} and \mathcal{L} to have the +y-face of \mathcal{D} and the axis of symmetry of \mathcal{L} be aligned with the line segment joining x_0 and c_{target} respectively. The choice of parameters considers a rendezvous approach with the Sun behind the spacecraft, as the gateway flies near the apolune of the NRHO.

The exact computation of $\mathcal{K}'_i(k, k + T_{\text{safe}})$ based on polytopes [4] is unreliable, due to the complexity of the calculations involved in the considered problem setting. Therefore, we use the proposed approach for inner-approximating T_{safe} -RC set using constrained zonotopes to enforce abort-safety constraint. Specifically, we use Theorem 1 and Section 5.2 to compute constrained zonotopic, inner-approximations of $\mathcal{K}'_i(k, k + T_{\text{safe}})$, and then use big-M formulations to cast the disjunctive constraints in (45) as mixed-integer linear constraints.

Consider N_D constrained zonotopes $\{\mathcal{C}_i\}_{i=1}^{N_D}$ where $\mathcal{C}_i \subseteq \mathcal{K}'_i(k, k + T_{\text{safe}})$ for each $i \in \mathbb{N}_{[1:N_D]}$ and some $k \in \mathbb{N}_{[t:t+T_{\text{plan}}]}$. Using N_D auxiliary continuous variables $\xi_i \in \mathbb{R}^{N_{C,i}}$ and N_D auxiliary binary variables $\delta_i \in \{0, 1\}$, and for any sufficiently large $M > 0$, the following set of $2(n + N_{C,i}) + M_{C,i} + 1$ mixed-integer linear constraints is equivalent to the constraint $x_{k|t} \in \bigcup_{i=1}^{N_D} \mathcal{K}'_i(k, k + T_{\text{safe}})$ at any $k \in \mathbb{N}_{[t+1:t+T_{\text{plan}}]}$,

$$\begin{aligned}
& \forall i \in \mathbb{N}_{[1:N_D]}, \quad \|G_{C,i}\xi_i + c_{C,i} - x_{k|t}\|_{\infty} \leq M(1 - \delta_i) \\
& \forall i \in \mathbb{N}_{[1:N_D]}, \quad A_{C,i}\xi_i = b_{C,i}, \quad \|\xi_i\|_{\infty} \leq 1, \\
& \sum_{i=1}^{N_D} \delta_i \geq 1.
\end{aligned}$$

See [32] for more details on mixed-integer reformulations of disjunctive constraints. Similar mixed-integer constraints based on big-M can be used to encode the disjunctive constraint $x_{k|t} \in \bigcup_{i=1}^{N_D} \mathcal{H}_i^{\mathcal{C}}$ [32]. Thus, we can cast (45) as a mixed-integer quadratic program, and solve it by off-the-shelf solvers like GUROBI [28].

Using the sets defined in Section 5, we can also compute an abort-safe control $u_{k|t} = \pi_k(\hat{z}_{k|t})$ for the current state estimate $\hat{z}_{k|t}$ by solving the convex optimization problem,

$$\underset{u_{k|t}}{\text{minimize}} \quad J(u_{k|t}) \tag{46a}$$

$$\text{subject to} \quad u_{k|t} \in \mathcal{U}_{\text{off-nom}}, \tag{46b}$$

$$A_t \hat{z}_{k|t} + B_{k|t} u_{k|t} \in \mathcal{K}_{k+1-t}, \tag{46c}$$

where J is a user-specified, convex cost function on the abort-safe control (we choose $J = \|\cdot\|_2$ to minimize post-failure fuel consumption), $\{\mathcal{K}_s\}_{s=0}^{T_{\text{safe}}}$ is the sequence of sets obtained using Section 5.2 with $\mathcal{K}_{T_{\text{safe}}} = \mathcal{H}_i^{\mathcal{C}} \ominus \mathcal{E}_{\text{off-nom}}$ and $\mathcal{K}(t, T_{\text{safe}}, \mathcal{H}_i^{\mathcal{C}} \ominus \mathcal{E}_{\text{off-nom}}) = \mathcal{K}_0$, as prescribed in Proposition 6. We compute the corresponding adversarial disturbance

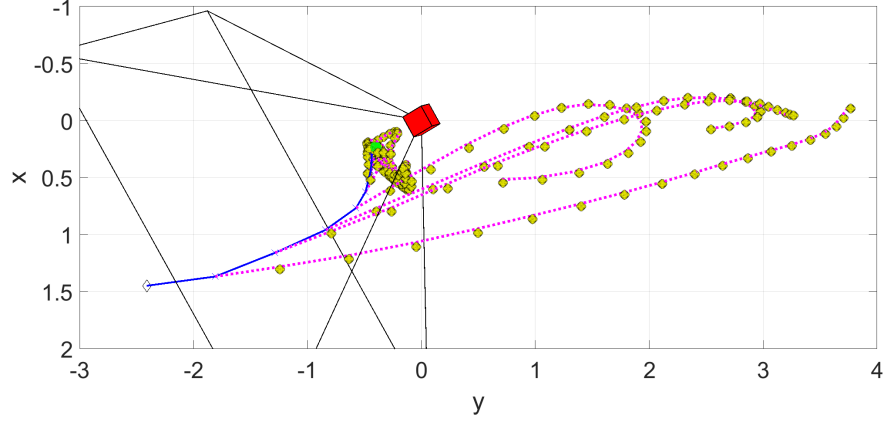


Figure 5: Designed nominal rendezvous trajectory along with the abort trajectories in case of failures at $t \in \mathbb{N}_{[1:T_{\text{sim}}]}$. The nominal trajectory starts at the initial state (diamond) and reaches the target set \mathcal{T} (green) in $T_{\text{sim}} = 10$ time steps, while staying within the line-of-sight cone \mathcal{L} (black). The abort-safety requirement curves the nominal trajectory away from the keep-out set (red) at all times. The abort trajectories stay outside the keep-out set, despite the presence of disturbances which are adversarially chosen according to (47).

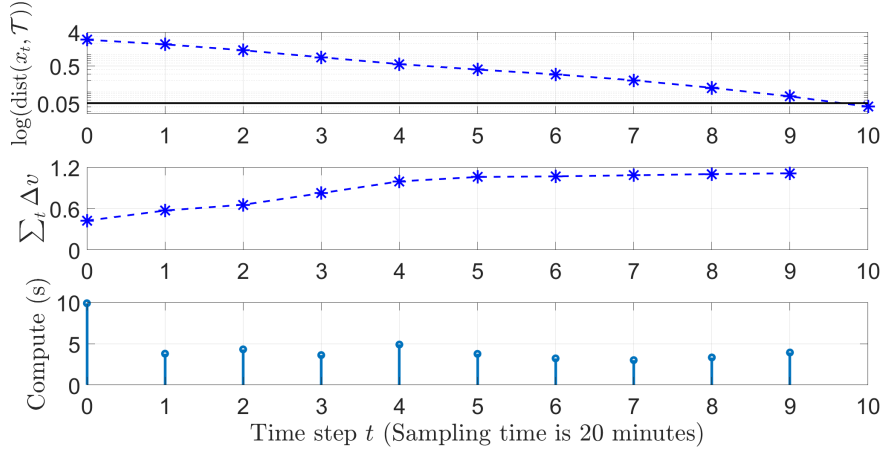


Figure 6: Evolution of the distance to the target (in log-scale) and cumulative Δv over the course of rendezvous, and computation time for each solution of (45).

$\phi_{k|t}$ by solving another convex optimization problem,

$$\min_{\hat{z}_{k+1|t}, \phi_{k|t}} \text{dist}(\hat{z}_{k+1|t}, \mathcal{D}) \quad (47a)$$

$$\text{s. t. } \phi_{k|t} \in \Phi_k, \quad (47b)$$

$$\hat{z}_{k+1|t} = A_t \hat{z}_{k|t} + B_{k|t} \pi_k(\hat{z}_{k|t}) + \phi_{k|t}. \quad (47c)$$

Here, (47) computes an adversarial disturbance that brings the next state estimate as close as possible to the keep-out set. By (47), we approximate the true worst-case disturbance sequence, whose exact computation would have required solving a two-player game, which is computationally difficult in six dimensions [5].

Figure 5 demonstrates the designed nominal rendezvous trajectory, which takes $T_{\text{sim}} = 10$ time steps (200 minutes) to reach \mathcal{T} with a total Δv of 1.07 m/s. The trajectory design required the computation of 385 18-step RC sets, and the set computation took a total of 7.53 seconds. Figure 5 also shows the designed abort-safe trajectories originating from each time step of the nominal rendezvous trajectory using the post-failure control (46) and adversarial disturbances (47), along with an outer-approximation of the one-step forward reach set $A_t \hat{z}_{k|t} + B_{k|t} \pi_k(\hat{z}_{k|t}) + \Phi_k$. As expected, the abort-safety requirement (43) is satisfied at all times $t \in \mathbb{N}_{[1:T_{\text{sim}}]}$. As the spacecraft approaches the target, we observe that the conservativeness of our enforcement of the abort-safety requirement (43) via Proposition 6 causes the

abort trajectories to cluster in front of the keep out set \mathcal{D} . In actual rendezvous missions, the spacecraft would receive a go/no-go decision for docking as it nears the target.

Figure 6 shows the evolution of the distance to the target set (in log-scale) and the cumulative Δv expended over the course of the rendezvous, as well as the computation time spent solving (45) at each time step $t \in \mathbb{N}_{[0:T_{\text{sim}}]}$. The rendezvous trajectory uses moderately high control inputs Δv initially to steer the spacecraft towards the target while satisfying the abort-safety requirements, and then utilizes the momentum to reach the target set with minimal additional control inputs, as expected. The rendezvous trajectory maintains abort-safety using the constrained zonotope-based constraints computed with the method proposed in this paper.

8 Conclusion

We presented novel theory and algorithms to approximate the Pontryagin difference between a constrained zonotopic minuend and a symmetric, convex, and compact subtrahend. For broad classes of subtrahends, our approach admits closed-form expressions for the inner-approximation. Then we used these algorithms for a tractable and scalable computation of an inner-(and outer-)approximation of the robust controllable set for discrete-time linear systems with additive disturbance sets that are symmetric, convex, and compact and subject to linear state and input constraints. We showed by numerical simulations that the proposed approach provides non-trivial inner-approximations of the RC sets with significantly shorter computation times than the previously published methods.

A current limitation of the proposed approach is that the subtrahend must be a symmetric set, which prevents us from stating a generic closed-form expression for the Pontryagin difference with a constrained zonotopic minuend, similar to (8) for a polytopic minuend. Our future work will investigate how to relax this assumption, and develop methods to apply the proposed algorithms in systems with low computational resources.

A Proofs

A.1 Proof of Proposition 1

Assume for contradiction that, for some representation of \mathcal{C} , some of the rows in G_C are linearly dependent. Then, there exists a vector $\alpha \in \mathbb{R}^n$, $\alpha \neq 0$ such that $\alpha^\top G_C = 0$. From (3), for every $x \in \mathcal{C}$, there exists $\xi \in \mathcal{B}_\infty(A_C, b_C)$ such that $G_C \xi = x - c_C$. Consequently, for any $x \in \mathcal{C}$, $\alpha^\top(x - c_C) = \alpha^\top G_C \xi = 0$, implying that $\mathcal{C} \subset \{x : \alpha^\top(x - c_C) = 0\}$. Thus, the affine dimension of \mathcal{C} is smaller than n , a contradiction since \mathcal{C} is full-dimensional. Thus, G_C has full row rank.

Let $[A'_C, b'_C]$ be a set of linearly independent $M'_C \leq M_C$ rows of the matrix $[A_C, b_C]$ such that $\text{rank}([A'_C, b'_C]) = \text{rank}([A_C, b_C])$. We show that $\mathcal{C} = (G_C, c_C, A'_C, b'_C)$. Without loss of generality, assume that $[A'_C, b'_C]$ are the first M'_C rows of $[A_C, b_C]$. By the choice of $[A'_C, b'_C]$, there exists $E \in \mathbb{R}^{(M_C - M'_C) \times M'_C}$ such that $[A_C, b_C] = [I_{M'_C}; E][A'_C, b'_C]$. Since the matrix $[I_{M'_C}; E]$ has full column rank, $[I_{M'_C}; E]y = 0$ if and only if $y = 0$. Consequently, the solution set $\{\xi : A_C \xi = b_C\} = \{\xi : A'_C \xi = b'_C\}$, since for any ξ such that $A_C \xi = b_C$, $[A_C, b_C][\xi; -1] = 0 \Leftrightarrow [I_{M'_C}; E][A'_C, b'_C][\xi; -1] = 0 \Leftrightarrow [A'_C, b'_C][\xi; -1] = 0$. Thus, $\mathcal{C} = (G_C, c_C, A_C, b_C) = (G_C, c_C, A'_C, b'_C)$.

Next, we observe that A'_C also has a full row rank of M'_C , using the following observations: 1) the matrix $[A'_C, b'_C]$ has full row rank of M'_C , 2) the set $\{\xi : A'_C \xi = b'_C\}$ is non-empty, and 3) b'_C lies in the column space of A'_C .

Finally, we show that the matrix $[G_C; A'_C]$ has full row rank to conclude that the constrained zonotope (G_C, c_C, A'_C, b'_C) is a MINROW representation of \mathcal{C} . Assume, for contradiction, that the matrix $[G_C; A'_C]$ has linearly dependent rows. In other words, there exists $\beta_1 \in \mathbb{R}^n$, $\beta_1 \neq 0$ and $\beta_2 \in \mathbb{R}^{M'_C}$, $\beta_2 \neq 0$ s.t.,

$$[\beta_1^\top, \beta_2^\top][G_C; A'_C] = 0 \equiv \beta_1^\top G_C + \beta_2^\top A'_C = 0. \quad (48)$$

We know $\beta_1^\top G_C \neq 0$ and $\beta_2^\top A'_C \neq 0$, since all rows of G_C are linearly independent, and all rows of A'_C are linearly independent. From (1b), for all $x \in \mathcal{C} = (G_C, c_C, A'_C, b'_C)$, there exists $\xi \in \mathbb{R}^{N_C}$ s.t.,

$$[G_C; A'_C]\xi = [x - c_C; b'_C] \text{ and } \|\xi\|_\infty \leq 1, \quad (49)$$

By (48) and (49), $\mathcal{C} \subset \{x : \beta_1^\top(x - c_C) + \beta_2^\top b'_C = 0\}$, which is a contradiction since \mathcal{C} is full-dimensional. Thus, all rows of $[G_C; A'_C]$ are linearly independent. \square

A.2 Proof of Proposition 2

Since \mathcal{C} is full-dimensional, it is non-empty. From (1b) and strong duality (via refined Slater's condition [21]),

$$\mathcal{C} = \left\{ x : \inf_{\substack{\xi \in \mathbb{R}^{N_C} \\ [G_C; A_C]\xi = [x - c_C; b_C]}} \|\xi\|_\infty \leq 1 \right\} \quad (50)$$

$$= \left\{ x : \sup_{\substack{\nu \in \mathbb{R}^{n+M_C} \\ \|[G_C; A_C]^\top \nu\|_1 \leq 1}} \nu^\top [x - c_C; b_C] \leq 1 \right\}. \quad (51)$$

For every $i \in \mathbb{N}_{[1:N_C]}$, define ν_i^* as the minimum-norm solution to $[G_C; A_C]^\top \nu = e_i$. Under Assumption 1, $[G_C; A_C]^\top$ has full column rank by Proposition 1, and ν_i^* is available in closed-form, where

$$\nu_i^* = ([G_C; A_C][G_C; A_C]^\top)^{-1} [G_C; A_C] e_i = ([G_C; A_C]^\dagger)^\top e_i,$$

for every $i \in \mathbb{N}_{[1:N_C]}$. Step 1 of Algorithm 2 (see (33)) rescales ν_i^* to ensure that $[G_C; A_C]^\top \nu_i^*$ has a unit ℓ_1 -norm to obtain v_i^\top . Thus, $\pm v_i^\top$ are feasible for (51) for every $i \in \mathbb{N}_{[1:N_C]}$, and using (51),

$$\mathcal{C} \subseteq \underbrace{\{x : \|V^\top [x - c_C; b_C]\|_\infty \leq 1\}}_{\mathcal{P} \triangleq \{x: Hx \leq k\}}, \quad (52)$$

with $V = [\nu_1^*; \nu_2^*; \dots; \nu_{N_C}^*]$. Since \mathcal{P} is a finite intersection of $2N_C$ hyperplanes in \mathbb{R}^n , \mathcal{P} is a convex polyhedron with $H \in \mathbb{R}^{(2N_C) \times n}$ and $k \in \mathbb{R}^{2N_C}$, as defined in Steps 2 and 3 of Algorithm 2. \square

A.3 Proof of Proposition 4

Since $[G_C; A_C]$ is invertible under Assumption 2, the optimal solution to (50) in Appendix A.2 has a closed-form expression $\xi^* = [G_C; A_C]^{-1} [x - c_C; b_C]$. Consequently,

$$\mathcal{C} = \{x : \|[G_C; A_C]^{-1} [x - c_C; b_C]\|_\infty \leq 1\} \quad (53)$$

$$= \left\{ x \mid \forall i \in \mathbb{N}_{[1:N_C]}, \forall \delta \in \{-1, 1\}, \delta e_i^\top [G_C; A_C]^{-1} [x - c_C; b_C] \leq 1 \right\}. \quad (54)$$

Here, v_i defined in Step 1 of Algorithm 2 also simplifies to $e_i^\top [G_C; A_C]^{-1}$ when $[G_C; A_C]$ is invertible [20, Sec. 11.5]. Thus, Algorithm 2 returns a convex polytope \mathcal{P} that coincides with (54) (thereby, equal to \mathcal{C}) under Assumption 2. \square

A.4 Proof of Proposition 5

Exactness of \mathcal{M}^+) Under Assumption 2, Algorithm 2 computes an exact polytopic representation of \mathcal{C} . Since the rest of steps of Algorithm 3 are exact, $\mathcal{M}^+ = \mathcal{C} \ominus \mathcal{S}$.

Exactness of \mathcal{M}^-) Since $[G_C; A_C]$ is invertible under Assumption 2, Γ prescribed by Theorem 2 is

$$\Gamma = [G_C; A_C]^{-1} [I_n; 0_{M_C \times n}], \quad (55)$$

by [20, Sec. 11.5].

We show that \mathcal{M} is an affine transformation of \mathcal{C}_L defined in the proof of Theorem 1. Specifically,

$$\begin{aligned} \mathcal{M} &= \mathcal{C} \ominus \mathcal{S} = \{x \mid \forall s \in \mathcal{S}_0, x + c_S + s \in \mathcal{C}\} \\ &= \left\{x \mid \forall s \in \mathcal{S}_0, \forall i \in \mathbb{N}_{[1:N_C]}, \forall \delta \in \{-1, 1\}, \delta e_i^\top [G_C; A_C]^{-1} [x + s + c_S - c_C; b_C] \leq 1\right\} \end{aligned} \quad (56)$$

$$= \left\{x \mid \forall s \in \mathcal{S}_0, \forall i \in \mathbb{N}_{[1:N_C]}, \forall \delta \in \{-1, 1\}, \delta e_i^\top \left(\Gamma x + \Gamma s + [G_C; A_C]^{-1} [-c_{M-}; b_C] \right) \leq 1\right\} \quad (57)$$

$$= \left\{x \mid \forall i \in \mathbb{N}_{[1:N_C]}, \forall \delta \in \{-1, 1\}, \delta e_i^\top \left(\Gamma x + [G_C; A_C]^{-1} [-c_{M-}; b_C] \right) \leq 1 - \rho_{\mathcal{S}_0}(\Gamma^\top e_i)\right\} \quad (58)$$

$$= \left\{x \mid \xi \triangleq \Gamma x + [G_C; A_C]^{-1} [-c_{M-}; b_C], \forall i \in \mathbb{N}_{[1:N_C]}, \forall \delta \in \{-1, 1\}, \delta e_i^\top \xi \leq D_{ii}\right\} \quad (59)$$

$$= \left\{x \mid G_C \xi + c_{M-} = x, A_C \xi = b_C, \forall i \in \mathbb{N}_{[1:N_C]}, \forall \delta \in \{-1, 1\}, \delta e_i^\top \xi \leq D_{ii}\right\} \quad (60)$$

$$= \{G_C \xi + c_{M-} \mid A_C \xi = b_C, \forall i \in \mathbb{N}_{[1:N_C]}, |e_i^\top \xi| \leq D_{ii}\} = G_C \mathcal{C}_L + c_{M-} = \mathcal{M}^-. \quad (61)$$

Here, (56) follows from (6d) and (54) in Appendix A.3, (57) follows from (55), (58) follows from encoding the condition for all $s \in \mathcal{S}_0$ using the support function of \mathcal{S}_0 , (59) follows from the definition of D_{ii} in (19), (60) follows from expressing ξ as a solution of linear equations $[G_C; A_C]\xi = [x - c_{M-}; b_C]$ with invertible $[G_C; A_C]$, and (61) follows from the definition of \mathcal{C}_L in (28) (see the proof of Theorem 1). Consequently, under Assumption 2, Theorem 2 provides an exact characterization of $\mathcal{C} \ominus \mathcal{S}$. \square

A.5 Proof of Proposition 6

From [23, Thm. 2.1(iii)],

$$(\mathcal{U} \ominus \mathcal{V}) \oplus \mathcal{V} \subseteq \mathcal{U}. \quad (62)$$

Let a failure occur at some time $s \in \mathbb{N}$. Using (42) and (62), for some $i \in \mathbb{N}_{[1:N_D]}$, $x_s = \hat{z}_{s|s} \in \mathcal{K}(s, T_{\text{safe}}, \mathcal{H}_i^{\mathcal{G}} \ominus \mathcal{E}_{\text{off-nom}}) \ominus \mathcal{E}_{\text{off-nom}}$, which implies that $\hat{z}_{s|s} \in \mathcal{K}(s, T_{\text{safe}}, \mathcal{H}_i^{\mathcal{G}} \ominus \mathcal{E}_{\text{off-nom}})$. From Definition 2, for every time step $k \in \mathbb{N}_{[s:s+T_{\text{safe}}]}$, there exists a feedback law $\pi_k \in \Pi$ such that $u_{k|s} = \pi_k(\hat{z}_{k|s}) \in \mathcal{U}_{\text{off-nom}}$ steers the state estimate according to the dynamics (41) to satisfy $\hat{z}_{k|s} \in \mathcal{H}_i^{\mathcal{G}} \ominus \mathcal{E}_{\text{off-nom}}$, irrespective of the disturbance $\phi_{k|s} \in \Phi_k$. By (42) and (62), $\hat{z}_{k|s} \in \mathcal{H}_i^{\mathcal{G}} \ominus \mathcal{E}_{\text{off-nom}}$ implies that the true post-failure state $z_{k|s} \in \mathcal{H}_i^{\mathcal{G}}$ (and thereby, $z_{k|s} \notin \mathcal{D}$) for all $k \in \mathbb{N}_{[s:s+T_{\text{safe}}]}$, which completes the proof.

References

- [1] W. Langson, I. Chrysoschoos, S. Raković, and D. Q. Mayne, “Robust model predictive control using tubes,” *Automatica*, vol. 40, no. 1, pp. 125–133, 2004.
- [2] D. Mayne, M. Seron, and S. Raković, “Robust model predictive control of constrained linear systems with bounded disturbances,” *Automatica*, vol. 41, no. 2, pp. 219–224, 2005.
- [3] F. Borrelli, A. Bemporad, and M. Morari, *Predictive control for linear and hybrid systems*. Cambridge Univ. Press, 2017.
- [4] M. Herceg, M. Kvasnica, C. Jones, and M. Morari, “Multi-Parametric Toolbox 3.0,” in *Proc. Euro. Ctrl. Conf.*, 2013.
- [5] D. Bertsekas and I. Rhodes, “On the minimax reachability of target sets and target tubes,” *Automatica*, vol. 7, pp. 233–247, 1971.
- [6] J. Scott, D. Raimondo, G. Marseglia, and R. Braatz, “Constrained zonotopes: A new tool for set-based estimation and fault detection,” *Automatica*, vol. 69, pp. 126–136, 2016.
- [7] V. Raghuraman and J. Koeln, “Set operations and order reductions for constrained zonotopes,” *Automatica*, vol. 139, 2022.
- [8] F. Gruber and M. Althoff, “Scalable robust safety filter with unknown disturbance set,” *IEEE Trans. Auto. Ctrl.*, vol. 68, no. 12, pp. 7756–7770, 2023.
- [9] L. Yang, H. Zhang, J. Jeannin, and N. Ozay, “Efficient backward reachability using the Minkowski difference of constrained zonotopes,” *IEEE Trans. Comp.-Aided Design Integ. Circ. Syst.*, vol. 41, no. 11, pp. 3969–3980, 2022.

- [10] J. Gleason, A. Vinod, and M. Oishi, “Lagrangian approximations for stochastic reachability of a target tube,” *Automatica*, vol. 125, 2021.
- [11] A. Vinod, A. Weiss, and S. Di Cairano, “Abort-safe spacecraft rendezvous under stochastic actuation and navigation uncertainty,” in *Proc. Conf. Dec. & Ctrl.*, 2021.
- [12] A. Vinod, J. Gleason, and M. Oishi, “SReachTools: a MATLAB stochastic reachability toolbox,” in *Proc. Hybrid Syst.: Comp. & Ctrl.*, pp. 33–38, 2019.
- [13] D. Marsillach, S. Di Cairano, and A. Weiss, “Abort-safe spacecraft rendezvous on elliptic orbits,” *IEEE. Trans. Ctrl. Syst. Tech.*, vol. 31, pp. 1133 – 1148, 2022.
- [14] H. Ahn, K. Berntorp, P. Inani, A. Ram, and S. Di Cairano, “Reachability-based decision-making for autonomous driving: Theory and experiments,” *IEEE. Trans. Ctrl. Syst. Tech.*, vol. 29, no. 5, pp. 1907–1921, 2020.
- [15] F. Blanchini and S. Miani, *Set-theoretic analysis of dynamic systems*. Springer International Publishing, 2015.
- [16] N. Malone, H. Chiang, K. Lesser, M. Oishi, and L. Tapia, “Hybrid dynamic moving obstacle avoidance using a stochastic reachable set-based potential field,” *IEEE Trans. Rob.*, vol. 33, no. 5, pp. 1124–1138, 2017.
- [17] C. Jones, E. Kerrigan, and J. Maciejowski, “On polyhedral projection and parametric programming,” *J. Opt. Theory App.*, vol. 138, pp. 207–220, 2008.
- [18] NASA, “Lunar gateway,” 2023. <https://www.nasa.gov/mission/gateway/> (Last accessed: 2023).
- [19] M. Althoff, “An introduction to CORA,” in *Proc. App. Verif. Cont. Hybrid Syst.*, pp. 120–151, December 2015.
- [20] S. Boyd and L. Vandenberghe, *Introduction to Applied Linear Algebra: Vectors, Matrices, and Least Squares*. Cambridge Univ. Press, 2018.
- [21] S. Boyd and L. Vandenberghe, *Convex optimization*. Cambridge Univ. Press, 2004.
- [22] A. Girard and C. Guernic, “Efficient reachability analysis for linear systems using support functions,” *IFAC Proc. Vol.*, vol. 41, no. 2, pp. 8966–8971, 2008.
- [23] I. Kolmanovsky and E. Gilbert, “Theory and computation of disturbance invariant sets for discrete-time linear systems,” *Math. Prob. in Engg.*, vol. 4, pp. 317–367, 1998.
- [24] S. Sadraddini and R. Tedrake, “Linear encodings for polytope containment problems,” in *Proc. Conf. Dec. & Ctrl.*, pp. 4367–4372, IEEE, 2019.
- [25] A. Kopetzki, B. Schürmann, and M. Althoff, “Methods for order reduction of zonotopes,” in *Proc. Conf. Dec. & Ctrl.*, pp. 5626–5633, IEEE, 2017.
- [26] J. Lofberg, “YALMIP: A toolbox for modeling and optimization in MATLAB,” in *IEEE Intn’l Conf. Rob. Autom.*, pp. 284–289, 2004.
- [27] MOSEK, *The MOSEK optimization toolbox for MATLAB manual. Version 10.0.*, 2022.
- [28] Gurobi Opt., LLC, “Gurobi Optimizer Reference Manual.” <https://www.gurobi.com> (Last accessed: 2023).
- [29] D. Marsillach, S. Di Cairano, U. Kalabić, and A. Weiss, “Fail-safe spacecraft rendezvous on near-rectilinear halo orbits,” in *Proc. Amer. Ctrl. Conf.*, pp. 2980–2985, IEEE, 2021.
- [30] V. Muralidharan, A. Weiss, and U. Kalabic, “Control strategy for long-term station-keeping on near-rectilinear halo orbits,” in *AIAA Scitech*, p. 1459, 2020.
- [31] W. Fehse, *Automated rendezvous and docking of spacecraft*, vol. 16. Cambridge Univ. Press, 2003.
- [32] A. Bemporad and M. Morari, “Control of systems integrating logic, dynamics, and constraints,” *Automatica*, vol. 35, 1999.